April 2015

Feel the Burn: Investigating New Sensitizers for Hybrid Dye-Sensitized Solar Cells

Ana Stella Mateo
Worcester Polytechnic Institute

Edwin Nicholas McGlew
Worcester Polytechnic Institute

Sarah Elizabeth Quatieri
Worcester Polytechnic Institute

Investigating New Sensitizers for Hybrid Dye-Sensitized Solar Cells

A Major Qualifying Project Report
Submitted to the Faculty of
WORCESTER POLYTECHNIC INSTITUTE
In partial fulfillment of the requirements for the
Degree of Bachelor of Science in Chemistry

Written by:

Ana Mateo
Edwin McGlew
Sarah Quatieri

Approved by:
Professor Drew Brodeur. Chemistry Major Advisor

Date: April 30th, 2015

Table of Contents

Table of Figures

List of Tables

Acknowledgements

We would like to thank Professor Drew Brodeur, for his patience, support, and expertise throughout this project. Most importantly, we would like to thank him for giving us such a wonderful opportunity to work with him on this project. We would also like to thank Professor Marion Emmert and her PhD student Kathleen Field for permitting us to use her lab space and equipment, as well as Professor Destin Heilman for his continued support.

Abstract

Fossil fuel depletion, greenhouse gas emission, and the increase in energy demand have fueled the need for solar power research. Hybrid dye-sensitized solar cells have shown promise due to their simplicity and low cost. Current research revolves around the utilization of nontraditional metal free organic compounds as part of these three component systems. This project investigates the effects that active organic sunscreen ingredients, which are known for broad UVA and UVB absorption, could have on solar cells when used as the light absorbing component. When normalized, the percent decrease in voltage was the same for each compound in varying solvents. The measured cell output was consistent with the amplitude of UV-absorbance of equimolar solutions. All components stayed at a relatively steady state under UV light up to 48 hours, significantly longer than the lasting effects of sunscreen. Synthetic changes on oxybenzone to form imine compounds showed improved voltage in two of the three solvents and similar overall stability. Results suggest that these active ingredients could be potential replacements for current sensitizers, and that additional synthetic functional changes as well as solvent optimization could continue to improve cell potential and long term stability.

1. Introduction

As fossil fuels are continually depleted, new sources of electricity are imperative for the continual use of energy at its current rate of consumption. Renewable energy is a necessity to avoid the inevitable energy crisis that would be faced as current sources are exhausted. Solar energy is one of the most researched forms of alternative energy since sunlight will continue to strike the surface of the planet every day, so it is logical to capitalize on the energy offered in the form of natural light.

While silicon wafer solar panels are effective and widely available, they are an expensive investment. Silicon solar panels are made from single-crystal wafers in order to prevent scattering within each cell. The costs of production, as well as the costs of potential failure to produce the wafers, are reflected in the price of the finished product. Thus, while solar energy is currently available at the consumer level, the cost per efficiency ratio leaves room for improvement.

To combat the price inherent to inorganic solar cells, methods for organic photovoltaic materials were investigated. While much cheaper and easier to produce, the organic cells were also significantly less efficient than already existing inorganic systems. In order to find a cheap cell that still converts light to electricity efficiently, hybrid cells were born. Hybrid cells combine advantages of inorganic and organic systems, using the organic component to absorb light and an inorganic semiconductor to drive the movement of electrons through the circuit. One of the simplest and most versatile types of hybrid solar cells is the dye-sensitized solar cell. Dye-sensitized solar cells contain three main and variable components: an organic dye, an inorganic semiconductor, and an electrolyte to replenish electrons lost by the organic dye. Generally, titanium dioxide is used as the semiconductor and iodide/triiodide is used as the electrolyte. Therefore, the organic component is the layer that can most easily be changed and tested for efficiency without having drastic effects on the cells' cost.

Many kinds of dyes have been tested for effectiveness in dye-sensitized solar cells. These include black Ru terpyridines (Kalyanasundaram & Grätzel, 1997), indoline and coumarin dyes, and various porphyrin derivatives, which are structurally similar to chlorophyll (Officer & Grätzel, 2007). All of these compounds are dyes that absorb light in the visible spectrum. However, the earth is irradiated with more than just visible light frequencies. This leaves a large portion of the

electromagnetic spectrum unaccounted for in terms of light absorbing compounds used to convert photons into electricity.

The goal of this project was to test the active ingredients of sunscreens as the photosensitizing component, or 'dye', in dye-sensitized solar cells. This was to determine if the existing, common compounds used for UV light absorbance or close derivatives would be viable for use as the sensitizing agent. The data collected indicate that organic compounds absorbing in the UV spectrum are viable option for photosensitization of dye-sensitized solar cells. With further consideration in solvent optimization and functional changes, derivatives from sunscreen active ingredients have the potential to make great sensitizers.

2. Background

Alternative energy is one of the most relevant scientific topics today. Currently there is a research focus on renewable energy specifically in the form of solar energy and photovoltaic devices. Hybrid dye-sensitized solar cells fall into a third generation of photovoltaic devices. To understand why these devices are so important, it is critical to look at the way in which they work as well as the current trend in design. The optimization of these devices creates great potential in the future of energy production.

2.1 Solar Energy

For decades, humans have depended on energy for survival. Industrial and technological growth has been possible due to proper utilization of energy (Lee, Speight, & Loyalka, 2007). Due to society's dependence on energy, the world energy consumption has increased. Some of the reasons for the drastic increase are: enhancement of quality of life, population increase, industrialization, rapid economic growth of developing countries, and increased transportation of people and goods (Lee et al., 2007).

The current world energy consumption is 4.1×10^{20} joules (J), which is equivalent to 13×10^{12} watts (W) (13 terawatt) per year (Nault, 2005). Studies show that the world's population is increasing at such high rates that it is estimated to double every century (Nathan, Crabtree, Nozik, Wasielewski, & Alivisatos). The wealthy commercial economy alone, which accounts for 25% of the world's population, currently consumes 75% of the world's energy supply (Dincer, 2000). However, our primary sources of energy are depleting while the energy demand is expected to increase by 3 times as much by 2050 (Dincer, 2000).

2.1.1 Non-Renewable Resources

Currently, the world's primary energy resources are non-renewable. These resources, which include coal, petroleum, and natural gas, are limited and decreasing in supply. While attempts have been made to utilize other resources, sufficient progress has not been made. In the U.S., coal, petroleum, and natural gas combined account for 82% of the energy consumption. These resources are limited and decreasing in supply.

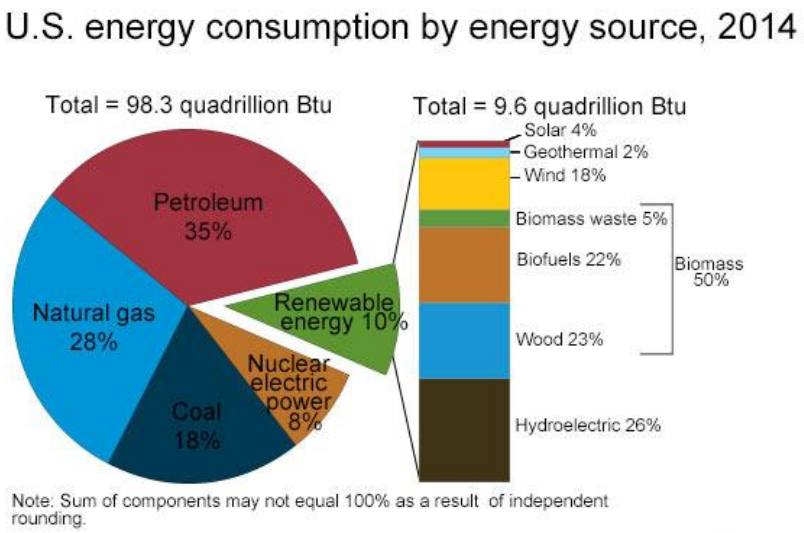

Figure 1: U.S. Energy Consumption, 2014 (U.S. Energy Information Administration)

Not only are the supplies of these resources decreasing, but there is also a pressing need to change energy supply due to the environmental concerns. These non-renewable resources have been associated with acid rain, ozone depletion, and the greenhouse effect.

Acid rain is caused by the emission of sulfur dioxide (SO_2) and nitrogen oxides (NO_x) from the combustion of fossil fuels (Dincer, 2000). These emissions react with oxygen and water in the atmosphere, increasing the amount of sulfuric and nitric acids in the atmosphere. Coal, transportation vehicles, and high sulfur fuels are the main contributing factors to the formation of acid rain. Acid rain causes acidification of lakes, streams, and ground water. It contributes to plant toxicity, damage to aquatic animals, deterioration of buildings, and much more (Dincer, 2000).

The ozone present in the stratosphere plays a crucial role in our daily lives. One of its major roles is to serve as a shield from harmful radiation such as ultraviolet and infrared. CFCs (chlorinated and fluorinated organic compounds) and nitrogen oxides (NO_x) are the main cause of the ozone layer diminishment (Dincer, 2000). This depletion causes harmful radiation to reach the ground and have detrimental effects on people's health and the environment.

The greenhouse effect is the term used to refer to the rise in the earth's surface temperature. This rise is caused by excess CO_2 and other gases referred to as greenhouse gases (CH_4, CFCs, Halons, N_2O, ozone, and peroxyacetylnitrate) that are produced by industrial and domestic activities (Dincer, 2000). These gases absorb the earth's thermal radiation resulting in

an increase in the average surface temperature, which has increased 0.6°C over the last century (Dincer, 2000).

2.1.2 Renewable Resources

Due to the increasing needs of energy and the negative effects associated with non-renewable resources, future implementations of alternative energy sources are crucial. In the U.S., renewable energy currently accounts for only 10% of the energy consumed. If our attempts to convert to renewable energy are successful, by 2050 the CO_2 levels could be reduced by 75% compared to those in 1985 (Johansson & Burnham, 1993).

There has been active research exploring renewable energy sources for decades. Some of these alternative energy sources include wind, hydropower, geothermal, and solar energies. Wind energy consists of the conversion of the rotation of turbine blades into electrical currents by an electric generator. Wind energy can produce electricity at a cost similar to that of coal and nuclear energy (Burton, Jenkins, Sharpe, & Bossanyi, 2011). However, the wind energy output has been estimated at 2-4 TW. Hydropower, which is the energy generated from the movement of rivers and oceans has been estimated to give about 2 TW of energy. These two energy sources would provide less than 30% of the current yearly energy needed (Nathan et al.). Geothermal energy comes from heat stored in the Earth's crust, partly from the formation of the planet and partly from radioactive decay of minerals. Geothermal energy would seem to be promising as it can generate 12 TW of energy. However, of these 12 TW only a small fraction could be extracted for energy purposes (Nathan et al.).

Solar energy is the conversion of sunlight into electricity or heat. It is the cleanest and most abundant renewable resource as it is obtained from sunlight (Foster, Ghassemi, & Cota, 2009). Solar energy can provide approximately 120,000 TW of energy, which is ten thousand times or more than other renewable resources (Nathan et al.). These two factors have attracted the attention of researchers worldwide. However, the cost of this form of energy tends to be higher due to the variation in availability caused by the day-night cycle and the changes in season. This variation makes storing energy a requirement, therefore increasing the cost (Sukhatme & Sukhatme, 1996).

There are several ways to collect solar energy: passive solar, concentrating solar power, solar heating and cooling, and photovoltaic (Dincer, 2000). In recent years, great strides have been made in the area of photovoltaic solar cells as a renewable energy source; however, there is room for improvement.

2.2 Solar Cells

There is an ever growing need for new renewable alternative energy resources. While many first generation solar cells are currently available commercially, second and third generation cells have the potential to become a cheaper more efficient option in years to come. To understand both the advantages and feasibility of these new devices it is important to understand the differences between them. Hybrid solar cells have the potential to become household items that can revolutionize the energy industry if optimized to their full potential.

2.2.1. Overview

Solar cells are devices that convert light into an electrical current that can be stored and used as energy. Semiconductors that exhibit the photovoltaic effect absorb photons to transfer electrons from the valence band to the conduction band, causing accumulation of voltage between two electrodes. These mobile electrons can then be led through a circuit to fill in the 'holes' left in the semiconductor material when the electron was transferred into the conduction band (Brabec et al, 2001).

2.2.2 Spectral Data

Terrestrial data of solar irradiance shows that most of the sunlight received on the Earth's surface consists of wavelengths shorter than 1100 nm. Longer wavelengths are mostly absorbed or scattered by molecules and particles in the atmosphere before arriving at the surface. As such, an effective semiconductor will have a band gap that allows for the bulk of these wavelengths to be absorbed (King et al, 1997).

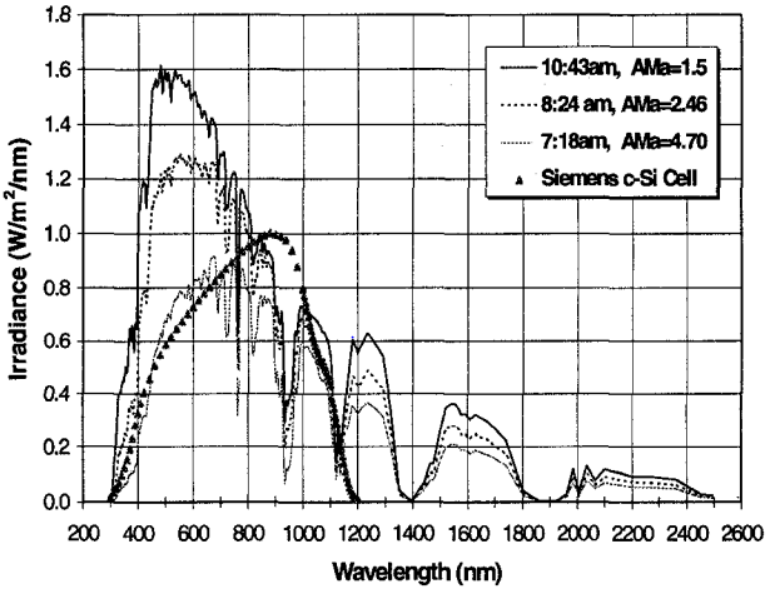

Figure 2: Relative Solar Spectral Response (King, Kratochvil, & Boyson, 1997)

Silicon solar cells have a band gap of 1.12 eV. This band gap allows these cells to absorb wavelengths shorter than 1100 nm, as such wavelengths have energy higher than 1.12 eV. As this accounts for most of the solar irradiation wavelengths that penetrate the atmosphere, silicon cells are well suited to absorb sunlight on the surface of Earth. The efficacy of future solar cell technology will be dependent upon the cells ability to absorb light at these critical wavelengths.

2.2.3 Structure and Mechanism

Standard inorganic solar cells consist of three main structures: a semiconductor body, front and rear contacts, and a circuit that connects the front to the rear contact.

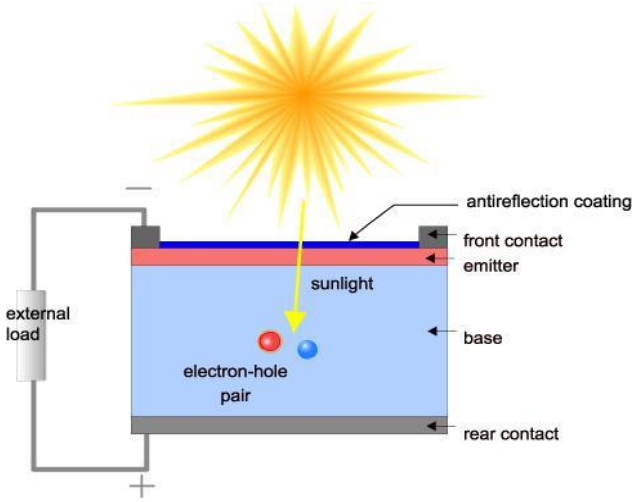

Figure 3: Structure of Standard Inorganic Solar Cell (Gunaicha, 2012)

Semiconductors are materials that exhibit electrical properties between those of classic conductors and insulators. While pure semiconductors exhibit resistivity, they can be doped with impurities to create alloys that exhibit adjustable electrical properties for unique applications. For solar cells, semiconductors can be doped with two different impurities to create N type (electron-rich) or P type (electron-poor) alloys. For example, a solar cell that uses silicon as a semiconductor could be doped with phosphorus to create an N-type semiconductor or with boron to create a P-type semiconductor (Seale, 2003). A doped semiconductor has unequal density of mobile electrons in the conduction band and mobile holes in the valence band. The difference of electron density at the P-N junction, where the electron-poor and the electron-rich parts of the semiconductor meet, provides a forward bias to make sure the flow of electricity runs in only one direction; without a P-N junction, the current could flow either way, which could cause a negative voltage.

With forward bias ensuring directionality of current, solar cells conduct displaced electrons through the front contact grid, through the external circuit where the electricity can do work, and then returns to the solar cell through the back contact.

When photons strike a solar cell, electrons are displaced from the semiconductor material. If conductors are attached to the positive and negative sides of the cell, these displaced electrons can be captured as an electric current (Ma et al, 2005). In order for an electron to be

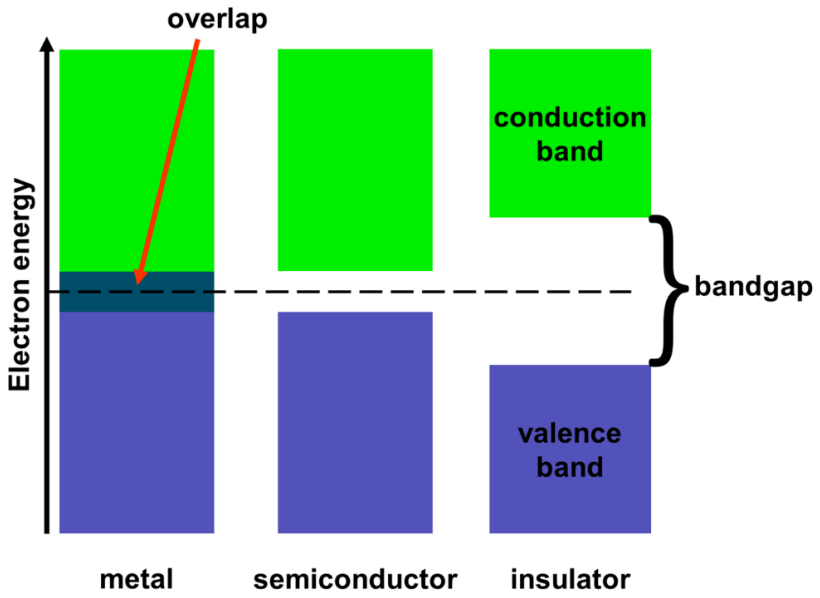

Figure 4: Difference in bandgaps between metal, semiconductor, and insulator materials (Strümpel et al, 2006)

displaced from the semiconductor, the energy of the photon must have at least as much energy as the band gap specific to the material. For example, the band gap of silicon cells is 1.12 eV, the cell must be hit by a wavelength smaller than 1100 nm for an electron to be displaced. If the photon has energy greater than 1.12 eV, the remaining energy is converted to heat (Strümpel et al., 2006).

2.2.4 Hybrid Solar Cells

Like standard inorganic solar cells, hybrid solar cells contain a photoactive layer, front and rear contacts, and a circuit that connects the front and rear contacts. However, unlike in standard inorganic solar cells, the photoactive layer of hybrid solar cells consists of two components: an organic material and a high electron transport material (Shaheen, Ginley, & Jabbour, 2005). These two components are combined in a heterojunction, with one material acting as the photon absorber and the other driving electron flow, providing directionality to the junction and thus to the circuit. In most cases, the organic layer is the photon absorbing component and the inorganic layer is the electron acceptor (Sariciftci, Smilowitz, Heeger, & Wudl, 2003). In order for an electron to move from the organic layer to the inorganic layer, an exciton generated by photon exposure must be separated from the organic layer. The energy required to separate an exciton is proportional to the difference between Lowest Unoccupied Molecular Orbitals (LUMOs) or conduction bands of the donor and acceptor materials. The acceptor material must have a lower LUMO than the polymer exciton donor for an electron to transfer (Saunders & Turner, 2008). To assist with exciton transfer between the organic and inorganic materials, there are several interface structure options to be explored depending on the materials in use.

The types of interfaces utilized in hybrid solar cells include mesoporous films, ordered lamellar films, and films of ordered nanostructures. A mesoporous film structure is comprised of a porous inorganic plate that is saturated with an organic surfactant. Ordered lamellar films have an alternating layout, with organic and inorganic compounds layered by electrodeposition-based self-assembly (Stupp, Herman, Goldberger, Chao, & Martin, 2011). Finally, ordered nanostructures of an inorganic material can be grown around the organic component, forming nanowires that can direct charge transport and minimize internal reflection and scattering (Weickert, Dunbar, Wiedemann, Hesse, & Schmidt-Mende, 2011). Each structure has a unique

advantage: ordered nanostructures provide the most directed pathways for electrons, lamellar films can self-assemble based on controlled solution chemistry, and mesoporous films are most easily and reliably produced.

The dye-sensitized solar cells that will be discussed in this paper are a specific branch of mesoporous film hybrid solar cells that use titania (TiO_2) as the inorganic material. Titania will act as a mesoporous inorganic layer, with each of the dyes tested acting as the saturating organic surfactant.

2.3 Dye-Sensitized Solar Cells

Dye-sensitized solar cells, also referred to in the literature as DSSCs or DSCs, have become an extremely popular subject of research in the area of solar energy. With energy needs doubling every century, research into these new renewable energy alternatives is increasing at an unprecedented rate. There is a large quantity of data on these devices and there are vast opportunities for the advancement of dye-sensitized solar cells particularly through optimization of their corresponding sensitizers. Before optimization of a variable component, we must first understand the other components and mechanistic properties of dye-sensitized solar cells.

2.3.1 Advantages

Dye-sensitized cells are currently in the running to become a third generation of solar cell technology. The goal for the third generation cells is large scale production at low cost, preferably less than $\$0.5/W_P$. This means very effective solar cells that are produced by techniques that permit facile mass production (Hagfeldt, Boschloo, Sun, Kloo, & Pettersson, 2010). The cells have the potential to become a cheap effective future energy producer. As described in Hagfelt's review, they also offer the following selling points:

- Low production cost and particularly interesting much lower investment costs compared with conventional PV technologies
- Design opportunities, such as, transparency and multi-color options (building integration, consumer products, etc.)
- Flexible, Lightweight

- Feedstock availability to reach terawatt scale
- Short energy payback time (< 1 year)
- Enhanced performance under real outdoor conditions (relatively better than competitors at diffuse light and higher temperatures)
- Bifacial cells capture light from all angles
- Outperforms competitors for indoor applications

(Hagfeldt et al., 2010)

This project will focus specifically on design opportunities and investigation and optimization of dye components from ingredients found within popular commercial consumer products. However, before testing and optimization it is critical to understand the mechanistic concepts of DSCs.

2.3.2 Dye-Sensitized Solar Cell Structure

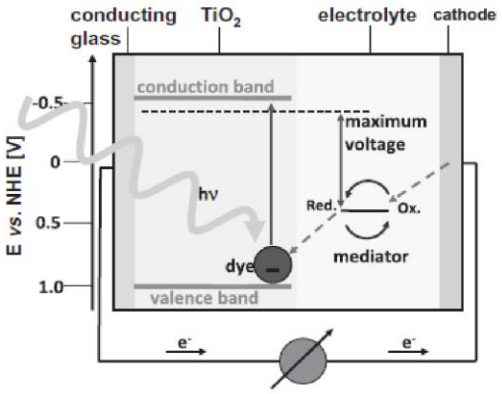

Figure 5: DSSC Operating Principles (Nazeeruddin, Baranoff, & Grätzel, 2011)

Dye-sensitized solar cells are slowly becoming a feasible competitor to 2nd generation p-n junction photovoltaic devices. The major difference in DSCs is that unlike other two component systems, which form a heterojunction, this one junction system allows electron transport, light absorption, and hole transport to be dealt with by separate components of the cell (Hardin, Snaith, & McGehee, 2012). Light will be absorbed by a sensitizer, in our case a metal free organic dye, attached to a wide band semiconductor. "Charge separation takes place at the interface via photo-induced electron injection from the dye into the conduction band of the solid. Carriers are transported in the conduction band of the semiconductor to the charge collector (Grätzel, 2003)." A photoexcited electron is transferred to the conduction band of a mesoporous oxide semiconductor layer during the absorption of light. The organic layer can then be restored

to its original state by an electrolyte. (Grätzel, 2003; Hardin et al., 2012; O'Regan & Gratzel, 1991). Titanium dioxide (titania -TiO_2) nanoparticles act as a mesoporous n-type photoanode and can increase the available surface area for dye attachment by an astounding factor of one thousand (Hardin et al., 2012; O'Regan & Gratzel, 1991).

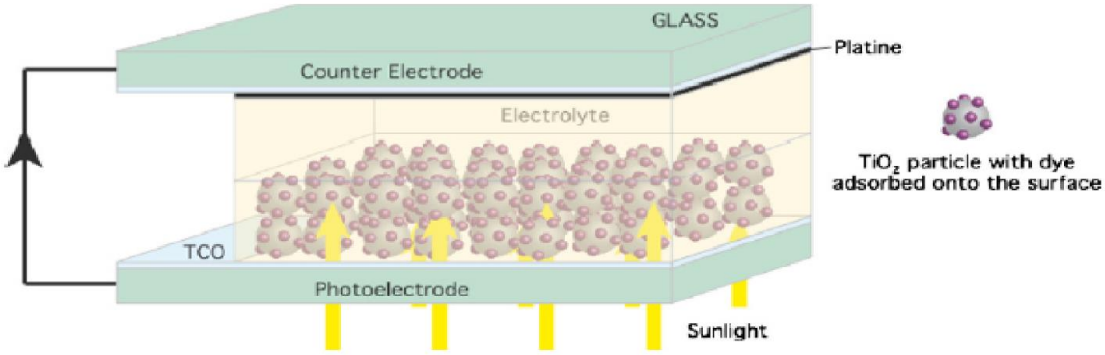

Figure 6: DSSC Schematic (Nazeeruddin et al., 2011)

As shown in figure on Nazeeruddin and Gratzel describe the DSSC by its five major components:

1. A mechanical support coated with Transparent Conductive Oxides
2. The semiconductor film, usually TiO_2
3. A sensitizer absorbed onto the surface of the semiconductor
4. An electrolyte containing a redox mediator
5. A counter electrode capable of regenerating the redox mediator like platine.

The previously mentioned schematic representation is similar to that of our dye-sensitized solar cells. Glass slides with a tin dioxide coating and graphite layer for component 1 and 5 will be used. Cells will be tested under fluorescent room lighting, UV light at 365 nm, and sunlight when possible. A variety of different oxides can be used in the construction of dye-sensitized solar cells; however, titanium dioxide is by far the most common. Its advantages for sensitized photochemistry include: low cost, wide availability, non-toxic, and biocompatible nature, and as such is used in many applications including industrial health care consumer products like sunscreens (Grätzel, 2003; O'Regan & Gratzel, 1991).

The electrolyte solution is KI/I2. “The iodide/triiodide system has been particularly successful in DSCs because of the slow recombination kinetics between electrons in the titania

with the oxidized dye and the triiodide in the electrolyte, which leads to long-lived electron lifetimes. The small size of the I^-/I_3^- redox components allows for relatively fast diffusion within the mesopores, and the two-electron system allows for a greater current to be passed for a given electrolyte concentration (Hardin et al., 2012)." These two components will remain constant during the entirety of our project. The final component, which completes this regenerative photovoltaic system and will be the variable component of this project, is the sensitizers absorbed onto the semiconductor surface.

2.4 Organic Dyes

Most current solar cells use inorganic or metal containing sensitizers as a light absorbing component. These metals are often rare earth metals that tend to be expensive, but also do not resonate with the idea of renewable energy since they have low natural abundance. Significant research is being done to utilize metal free organic compounds, which can provide a cheap alternative to the current metal dyes.

2.4.1 Advantages of Organics

The disadvantage found with inorganic or metal- containing dyes is their high expense and low natural abundance, especially with high efficiency rare earth metals like cadmium. Organic dyes have already proven to be a feasible alternative, though there is much more investigation to be done before they can be mass produced for industrial purposes.
Most research to date on commercially available photovoltaic technologies is based on inorganic materials. These inorganic materials are commonly high cost and their preparation requires high energy consuming methods. Organic photovoltaics could potentially avoid those problems in the future (Nazeeruddin et al., 2011). Right now groups of organic dyes with specific properties of interest have been synthesized and found to provide efficient solar conversion. However, they are still far from that of pure inorganic photovoltaic devices. One of the major problems is the narrow spectral bandwidths of organics compared to popular ruthenium or other metal ligand complexes (Hardin et al., 2012). Over the past decade, great strides have been made in both understanding and synthetically designing new dyes for use in DSCs (Hardin et al., 2012). In 2009, "the best organic DSSCs are currently running at power conversion efficiencies of 8–9 %

in liquid DSSCs, approximately 7 % in IL-DSSCs, and exceeding 4 % in solid-state cells (Mishra, Fischer, & Bäuerle, 2009).” These numbers have since been improving. While there are clear setbacks to pure organic solar cell components, the available potential for future synthetic advancements far outweigh any setbacks seen in the current year. As with most scientific concepts, with each backbone or major core there are thousands of possibilities still yet to be evaluated. The opportunity for optimization of low cost easily synthesized dyes is the driving force that organics are a viable and potential future competitor in the building of 3rd generation dye-sensitized solar cells.

2.4.2 Optimization of Dyes

As previously mentioned, metal-free organic dyes are often being designed and synthesized with the aim of replacing expensive ruthenium (II) complexes, but also to widen the scope of available sensitizers and to explore a new generation of solar cell research opportunities. As we continue to plan for the synthesis of new organic dyes, it is imperative to understand the optimal functional activity needed for efficient solar power conversions. For each compound multiple parameters play a role in the effectiveness of an organic compound to be classified as a good sensitizer. The efficiency and efficacy of DSCs depend on the nature of the photoelectrode, binding group of the dye, electrolyte, and mediating redox couple. The general backbone of a dye or sensitizer consists of a donor–acceptor-substituted π-conjugated “bridge” to which the anchoring group to the TiO_2 is attached or bound to the acceptor (Figure 7) (Hardin et al., 2012).

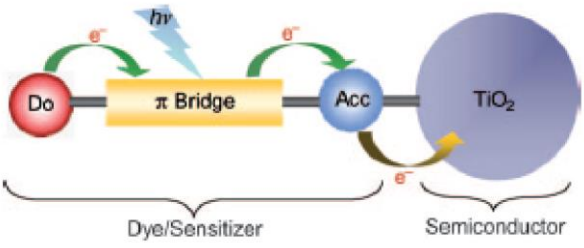

Figure 7: Dye Components

“The best dyes contain both electron-rich (donor) and electron-poor (acceptor) sections connected through a conjugated (pi) bridge. The electron-poor section is functionalized with an acidic binding group that couples the molecule to the oxide surface (Hardin et al., 2012).” These

groups are most often carboxylate or phosphonate groups that graft compounds to the semiconductor oxide surface. Photoexcitation causes an electron transfer from the donor to acceptor. Long alkyl chains are often attached to the backbone of a sensitizer to create a barrier between holes in the redox couple and electrons in the titania; this mechanism can inhibit detrimental recombination (Hardin et al., 2012).

Even taking into consideration these parameters, researchers still run into issues with the absorption bands of organic photovoltaics. Organic compounds often have narrow absorption bands in the visible region compared to ruthenium complexes. "One of the greatest opportunities for improving the efficiency of all types of DSC is to reduce the energy gap of the dyes so that more light in the spectral range of 650–940 nm can be absorbed. However, finding one dye that absorbs strongly all the way from 350–940 nm is extremely difficult. Typically, the peak absorption coefficient and spectral width of a dye are inversely related to each other. The most promising strategy for harvesting the whole spectrum is to use a combination of visible- and NIR-absorbing dyes (Hardin et al., 2012)." DSCs future potential in the photovoltaic market for a third generation solar cells will depend on our ability to increase power-conversion efficiencies and our ability of DSCs to be synthesized and constructed from abundant non-toxic materials (Hardin et al., 2012).

2.4.3 Natural Organics Sensitizers

Naturally occurring light absorbers can be found in a variety of produce, such as anthocyanins found in fruits like raspberries, cranberries, pomegranates, and blueberries. These fruits and their respective 100% organic juices have the potential to be used as dyes for initial baseline tests due to the abundance of anthocyanins they contain. These juices have been used by students and professional research scientists in academia and industry for production and design of DSCs. We will focus on blueberries since the juice is already widely available and its acidity will not compete with the approximately pH 3 suspension of titanium dioxide, which will be discussed further in the experimental section 3.1.1.

Anthocyanins have a general multi ring backbone. The all have a characteristic $C_6C_3C_6$ skeletal structure, common in flavonoids, and the anthocyanins' specific properties are

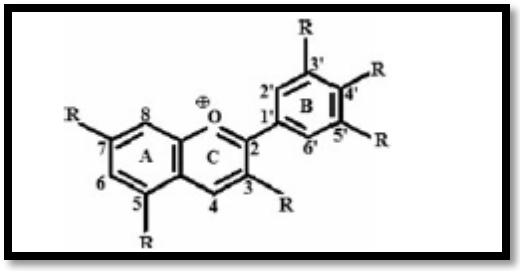

Figure 8: Anthocyanin Backbone

dependent upon the hydroxylation and methoxylation of this backbone (Routray & Orsat, 2011). The pi system in the backbone of these structures makes them great targets as a sensitizer in dye-sensitized solar cells. Anthocyanins generally absorb around 560 nm, however, it is different for each juice due to the variation in types of anthocyanins and their varying concentrations.

Table 1–Anthocyanins commonly present in blueberries, their structures, sugar moieties, and color.

Anthocyanin based on	Basic structure	R (Sugar moiety)	Color
Cyanidin		Galactose, Glucose, Arabinose	Orange-red
Delphinidin		Galactose, Glucose, Arabinose	Blue-red
Malvidin		Galactose, Glucose, Arabinose	Blue-red
Petunidin		Galactose, Glucose, Arabinose	Blue-red
Peonidin		Galactose, Glucose, Arabinose	Orange-red

Figure 9: Blueberry Anthocyanins (Routray & Orsat, 2011)

Figure 9 shows the multiple variations in anthocyanins in blueberry juice alone.

2.4.4 Sunscreen and UV Absorption

To date, there is currently no research involving the combination of sunscreen organic active ingredients and dye-sensitized solar cells. Due to the nature of sunscreen, it is safe to assume that active ingredients found in these commercially available products could potentially be used as viable sensitizers is DSCs. Active ingredients of sunscreen are proven to absorb three categories of UV light, UVB, UVA1, and UVA2. Light in the UVA1 range covers absorbance at 315 to 340 nanometers. UVA2 covers 340 to 400 nm and UVB wavelenghts of 280 to 315 nm.

FDA-approved*active sunscreen ingredient	Maximum FDA-approved concentration (%)	Peak absorption wavelength (nm)	Range of protection (nm)	Protection provided (UVB/UVA)
Inorganic				
Titanium dioxide	25.0	Varies	290-350	UVB, UVA2
Zinc oxide	25.0	Varies	290-400	UVB, UVA1
Organic UVB				
PABA	15.0	283	260-313	
Padimate O	8.0	311	290-315	
Octinoxate (octyl methoxycinnamates)	7.5	311	280-310	
Cinoxate	3.0	290	270-328	
Octisalate (octyl salicylate)	5.0	307	260-310	UVB
Homosalate	15.0	306	290-315	
Trolamine salicylate	12.0	260-355	269-320	
Octylocrylene	10.0	303	287-323	
Ensulizole (phenylbenzimidazole sulfonic acid)	4.0	310	290-340	
Organic UVA				
Oxybenzone	6.0	290, 325	270-350	UVB, UVA2
Sulisobenzone	10.0	366	250-380	UVB, UVA2
Dioxybenzone	3.0	352	206-380	UVB, UVA2
Meradimate (menthyl anthranilate)	5.0	336	200-380	UVA2
Avobenzone	3.0	360	310-400	UVA1, UVA2
Ecamsule (terephthalydene dicamphor sulfonic acid [Mexoryl SX])	10.0	345	295-390	UVA1, UVA2

*FDA approved as of Dec. 7, 2009.

Figure 10: FDA Approved Sunscreen Ingredients (Sambandan & Ratner, 2011)

Seventeen organic and inorganic materials are currently approved by the FDA (Figure 10) as sunscreen active ingredients. While this seems like a substantial amount, it pales in comparison to the 34 in Australia and 28 in the European Union (EU). Sunscreen ingredients are divided by their inorganic and organic nature, which are also classified as physical blockers and chemical absorbers, respectively (Sambandan & Ratner, 2011). “Inorganic sunscreen ingredients reflecting and scatter visible, UV, and infrared radiation. The major inorganic agents used today are zinc oxide and titanium oxide (see Figure 10), which are photostable and require a thick application to

achieve adequate reflection. Titanium dioxide provides UVB protection and emits a white tone because of its high refractive index (Sambandan & Ratner, 2011). Organic ingredients act by absorbing UVR and converting it to heat energy (see Figure 10). Salicylates like homosalate, octisalate, and trolamine are by far the weakest organic UVB agents. However, due to the safety of the products, they are often some of the most common ingredients found in commercial products and have much higher allowed percentages than their other organic counterparts (Sambandan & Ratner, 2011). Investigation in the use of these ingredients will be mainly on the most common organic chemical absorbers. Organic components are not found unaccompanied in sunscreen. Often there is a combination of ingredients to allow the sunscreens to be classified as broad spectrum covering most of the three UV categories of light. This classification is where SPF (sun protection factor) comes into play. "SPF is largely a measure of UVB protection. An SPF 15 sunscreen filters about 94% of UVB rays, whereas SPF 30 blocks about 97% (Sambandan & Ratner, 2011)." Broad spectrum products must combine both UVA and UVB filters.

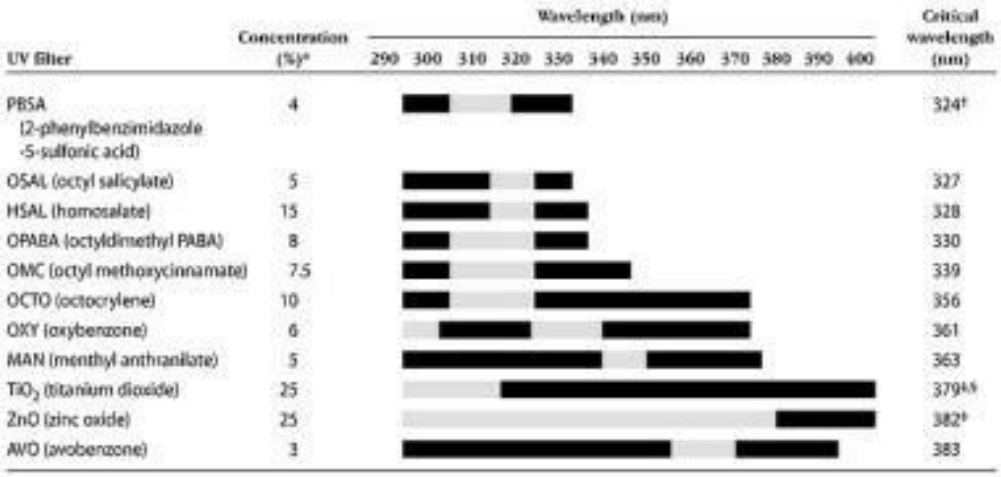

Figure 11: Sunscreen Ingredients Absorbance (Diffey, Tanner, Matts, & Nash, 2000)

Figure 11 shows the coverage of each of the 17 FDA approved sunscreen ingredients. After investigation of products commonly available, it was found that octisalate, homosalate, oxybenzone, avobenzone, octinoctate, and octocrylene were the most widely available and commonly used organic components.

Octisalate and homosalate are highly photostable compounds used as accompanying components that reduce photodegradation of photolabile sunscreen active ingredients. Their

hydrophobic nature also allows them to serve as solvents for other sunscreen components (Sambandan & Ratner, 2011). Benzophenones provide broad-spectrum UVB and UVA protection making them extremely beneficial. The only disadvantage to using benzophenones is that they are extremely photolabile and their oxidation can interrupt antioxidant systems. Oxybenzone is the most common benzophenone. However, avobenzone (butyl methoxydibenzoylmethane, Parsol 1789), a potent UVA filter, is also widely used and was the first FDA approved organic agent to effectively filter UVA1. However, it is highly photolabile (Sambandan & Ratner, 2011). In the same manner that organic dyes can be combined to improve efficiency of solar cells, sunscreen ingredients are combined for broader spectrum coverage as well as to stabilize certain photolabile compounds. "Avobenzone, a superior UVA blocker, can be combined with homosalate and octisalate, UVB filters, to yield broad-spectrum coverage. Because of the increased photolability of benzophenones and avobenzone, octocrylene is often added to improve sunscreen photostability with these agents (Sambandan & Ratner, 2011)."

Research suggests that due to their light absorbing properties and the synthetic opportunities for optimization, sunscreen active ingredients could prove to be good targets as sensitizers in dye-sensitized solar cells. They are already proven to absorb in ranges from 200-400 nm and with additional sensitizers or optimized functional groups could become a feasible new alternative to already available metal-free organic sensitizers.

3 Experimental

In this section, the experimental procedures executed by the team are explained in detail. These procedures include those for building the solar cells as well as those taken when considering and implementing a synthesis plan.

3.1 Building a Solar Cell

3.1.1 Suspension

The titanium dioxide (TiO_2) paste was prepared by mixing 6 grams of TiO_2 powder with 7 mL of acetic acid (pH 3.03). The acetic acid was slowly added in 1 mL increments while grinding the mixture using a mortar and a pestle for approximately 30 minutes until a smooth consistency was obtained. Once the acetic acid was added, 1.5 mL of surfactant (Triton X 100 diluted solution) was added to the paste and gently stirred.

3.1.2 Assembling the Cell

The conductive sides of the glass slides were determined by taking each slide's resistance with a multimeter. The conducting sides were observed to have a resistance ranging from 17-26 ohms. Two slides with the same initial resistance were used to make one cell. With the conductive side facing up, one slide was coated with graphite leaving about 0.5 cm on one side.

The conductive side of the other slide was coated with the TiO_2 suspension. Pieces of tape were placed on the slide to control the placement and thickness of the TiO_2 as shown in figure 12.

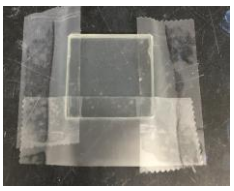

Figure 12: Solar cell coating preparation

A small amount of the TiO_2 suspension was placed on the slide and spread using a back and forth motion with a glass-stirring rod. Once an even layer was obtained, the tape was removed and the slide was immediately placed on a hot plate. The slide was heated until the hot plate reached 450 ^{o}C, at which time the TiO_2 layer was observed to turn brown and back to white as it cooled.

Once the slide had cooled, 200 µL of dye was added to the TiO_2 layer. The graphite coated slide and the TiO_2 slide were clamped together in an offset manner to allow the part of the uncoated sections to extend beyond both sides. Multiple drops of electrolyte solution (KI/I_2) were added between the two slides until the TiO_2 layer was covered by capillary action. Excess electrolyte was removed to ensure clips were not in contact with residual electrolyte.

The alligator clips of a multimeter were clamped to the uncoated sections that extended on the sides of the cell. The negative electrode was clamped to the slide with the TiO_2 layer while the positive electrode was clamped to the graphite coated slide. With this setup, the current and voltage of each cell were taken under room and UV light for consistent time points starting with the initial time to 14 days.

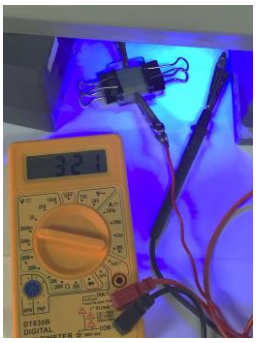

Figure 13: Solar cell under UV light

3.2 Active Sunscreen Ingredients

The five ingredients of interest were chosen based on their availability and the fact that they are five of the most common active ingredients across a variety of sunscreens or various brands and varying SPF values.

3.3 Synthesis Methodology

Oxybenzone, a common active sunscreen ingredient, shows great potential as a light absorbing component in dye-sensitized solar cells. Through synthetic functionalization cell performance was monitored to determine the effect of a functional carbonyl to imine change. Basic synthetic procedures were carried out to synthesize three separate compounds with oxybenzone as the starting material.

3.3.1 Synthesis Plan

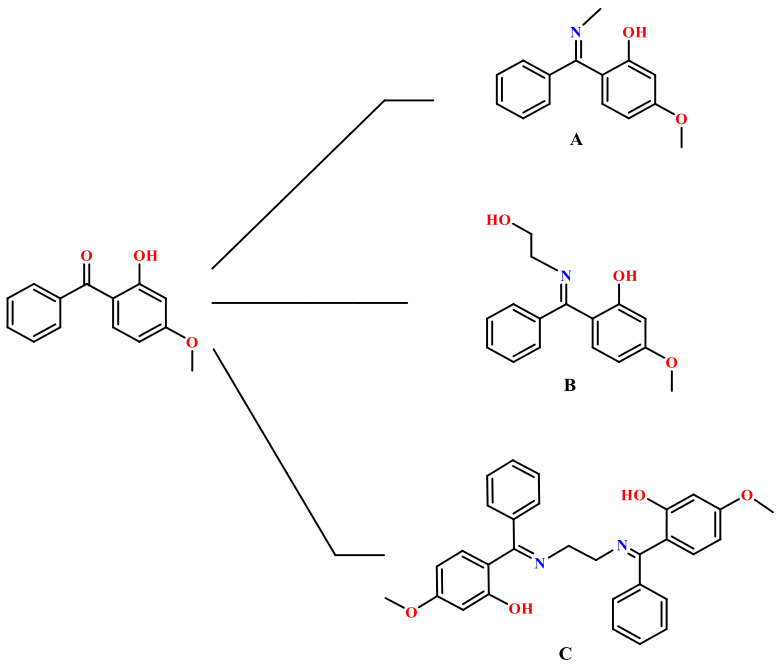

Figure 14: Schematic for functionalization of Oxybenzone

Oxybenzone was synthetically functionalized to produce compounds A, B, and C, by methods later described in the experimental procedures. The goal was to examine long term effects on cell performance due to functional change, specifically the change due to imine functionalization. Oxybenzone was one of the best absorbing components of the five ingredients, and the availability of starting material was the reason it was chosen for functionalization. Compound A could be made in a simple system in the absence of solution. Compounds B and C were synthesized by reflux and requiring only simple purification through column chromatography or washing, respectively.

3.3.2 Experimental Procedures

General Procedures:

Reagents, catalysts, ligands, and solvents were purchased reagent grade, checked by analytical methods before use, and used without further purification. ^{1}H NMR spectra were recorded on a Bruker AVANCE III 500 (500 MHz) NMR spectrometer. Chemical shifts are

reported in ppm (δ) relative to DMSO at 2.50. Thin- layer chromatography was performed on pre-coated silica gel plates and visualized under ultraviolet light. LC/MS data was obtained on an Agilent Technologies 6130 Quadruple LC/MS. Removal of solvent was carried out on a rotary evaporator at reduced pressure, unless noted otherwise.

*Synthesis of compound **(A)***

Solid oxybenzone was placed on one side of an H-Tube (2g, 0.009 mol) and 40% methylamine aq. solution (3mL) on the other. The H-tube was sealed immediately and allowed to sit at room temperature. After 22h, the pale yellow ketone was converted to a yellow solid. The solid was precipitated in dH2O (3mL) to produce the pure product. ^{1}H NMR (500MHz, CDCl3) δ 3.05 (s,3H), 3.79 (s, 3H), 6.08 (dd, J 2.6, 9.1 Hz, 1H), 6.38 (d, J 2.6 Hz, 1H), 6.63 (d, J 9.1 Hz, 1H), 7.25 (m, 2H), 7.52 (m, 3H); LC/MS 242.1 (M+1).

*Synthesis of compound **(B)***

Compound **B** was obtained by condensation of an oxybenzone (2g, 0.009 mol) with the ethanolamine (543 µL, 0.009 mol) under reflux in methanol for 3 hrs. The product was purified by column chromatography (2:1 Ethyl acetate/ Hexane). The product-containing fractions were concentrated to yield a yellow solid. ^{1}H NMR (500MHz, CDCl3) δ 3.48 (t, J 5,5 Hz, 2H), 3.82 (s, 3H), 3.88 (t, J 5.5 Hz, 2H), 6.18 (dd, J 2.6, 9.1 Hz, 1H), 6.44 (d, J 2.6 Hz, 1H), 6.69 (d, J 9.1 Hz, 1H), 7.26 (m, 2H), 7.52 (m, 3H); LCMS 272.1 (M+1).

*Synthesis of compound **(C)***

Compound C was prepared according to standard procedures for preparation of salen-type ligands. Reaction of 2-hydroxy-4-methoxybenzophenone (2.0g, 0.009 mol) and ethylenediamine (333 µL 0.005 mol) in refluxing isopropanol for 6 h afforded C as a pale yellow powder. The solution was cooled to r.t.,and the solid product was filtered off with suction, washed with isopropanol and dried in air. Yield 72%. ^{1}H NMR (500MHz, CDCl3) δ 3.53 (s,4H), 3.78 (s, 6H), 6.14 (dd, J 2.6, 9.1 Hz, 2H), 6.42 (d, J 2.6 Hz, 2H), 6.61 (d, J 9.1 Hz, 2H), 7.12 (m, 4H), 7.46 (m, 6H).

4 Results and Discussion

Results of this project exist in two main categories; spectral data and cell performance. In this section, spectral data is discussed and compared directly to cell performance given by graphical representation of voltage output for dye-sensitized solar cells over time. Clear trends are seen in the data sets that suggest that active ingredients are a viable option for use as sensitizers in DSSCs.

4.1 Spectral Data

Infrared and UV-Vis spectroscopy were used to determine spectral characteristics of the tested light absorbing components. IR was used to determine experimental limits of solar cell design while UV-Vis was utilized for both characterization and investigation of light absorbing components.

4.1.1 Infrared Spectroscopy

In order to determine the optimal amount of the organic component to apply to each cell, IR spectra were taken for successive amounts of each compound added to a cell. The optimal amount is enough to affect all active sites of the TiO_2 layer without excess molecules impeding light.

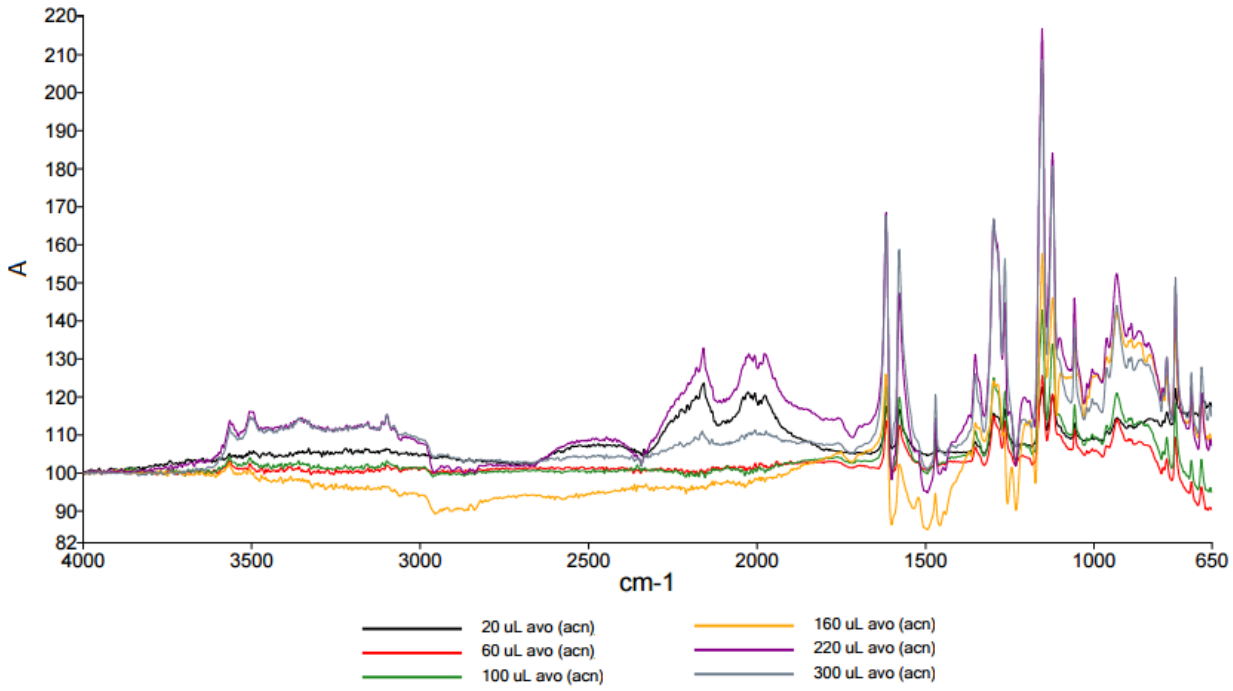

Figure 15a: Normalized IR spectra of Avobenzone

For the data collected from successive additions of 0.05 M solutions of avobenzone, octocrylene, and oxybenzone, the resulting spectra clearly showed that peaks increased proportionally with respect to amount of the organic compound added until the addition from 220 µL to 300 µL, at which point the change between peak amplitude became reduced by a significant margin compared to every spectrum other collected. Thus, around 200 µL of 0.05M compound was determined to be the saturation point of molecules on the TiO_2 active sites. Therefore, 200 µL of 0.05M solution were applied to each solar cell to optimize the amount of light absorbed by the organic component in each cell. Spectra of avobenzone are found in the figure above. The other two trials can be found in appendix A.

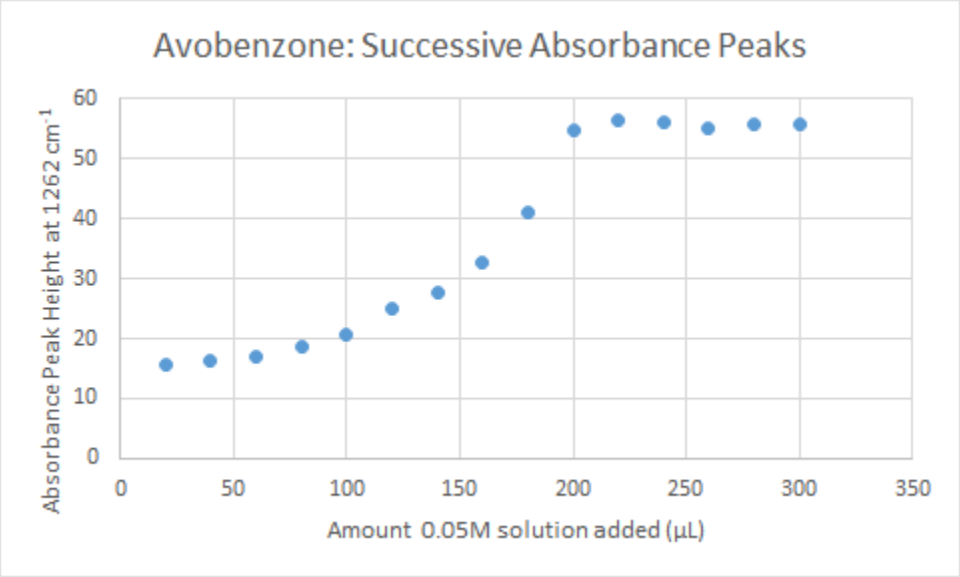

Figure 15b: Absorbance Peak Height after Successive Additions of 0.05M Avobenzone Solution

The organic solutions were not added beyond 200 µL to ensure that, while as many of the TiO_2 active sites were occupied as possible, there were not excess organic molecules blocking light from exciting the organic molecules attached to the TiO_2.

4.1.2 UV-Vis Spectroscopy

UV-Vis spectra were taken for all active ingredients as well as synthesized compounds in each of the three solvents: t-butanol, ethanol, and acetonitrile. Exactly 6 µL of each 0.5M solution of compounds was added to 3 mL of the respective solvent for UV-Vis trials. This concentration was kept consistent for every UV test.

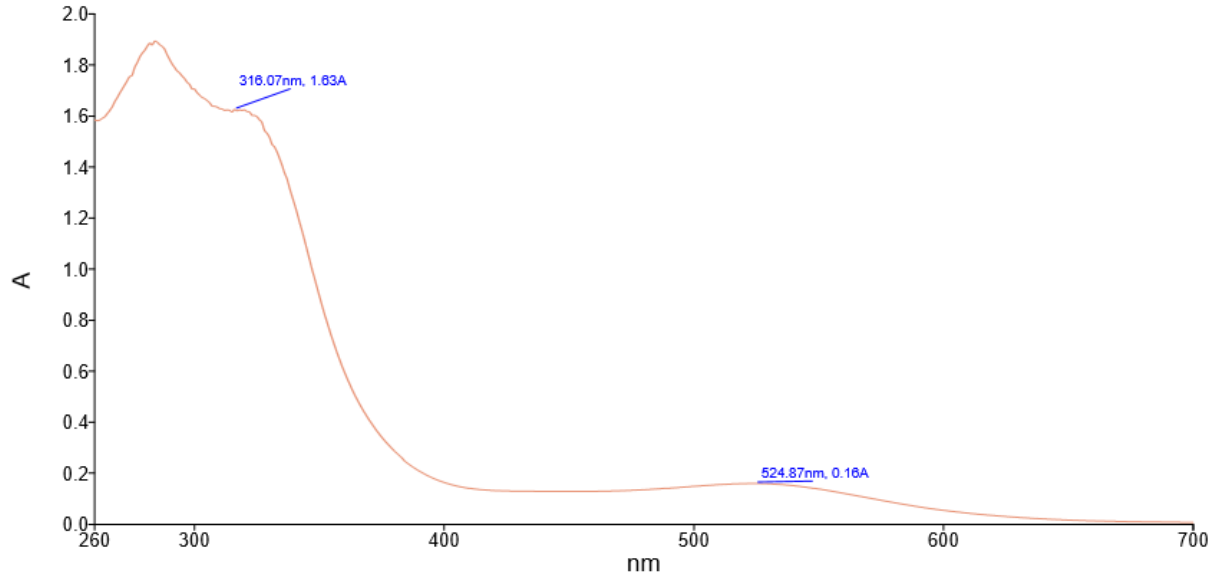

Figure 16: UV-Vis spectrum of blueberry juice

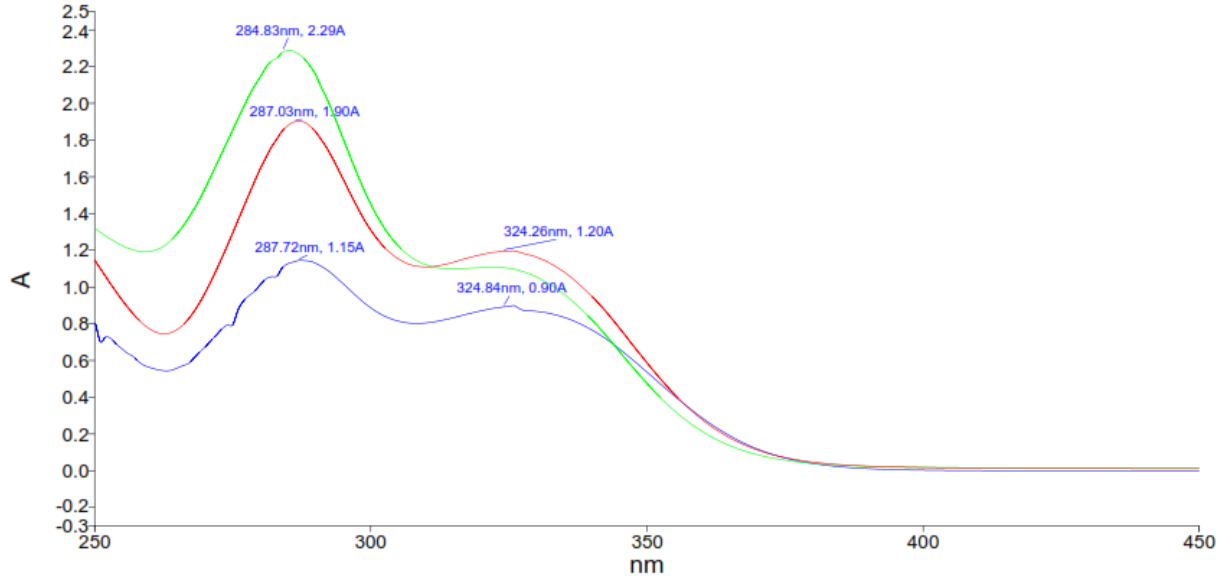

Figure 17: UV-Vis spectrum of Oxybenzone in acetonitrile (green), ethanol (red), and t-butanol (blue)

It can be seen that max wavelength values were consistent with literature values as seen in figure 11. The max wavelengths for avobenzone, oxybenzone, octisalate, homosalate, and octocrylene did not shift more than 5 nm when solvents were varied. It was however seen that the absorbance increased in amplitude. Oxybenzone spectra are shown in figure 17 and the remaining UV-Vis spectra can be referenced in appendix B.

4.2 Comparison of Voltage vs UV Vis Spectra

In order to see if there were any correlations between the absorbance and voltage output of each sunscreen organic ingredient and one of the synthesized compounds, UV-Vis spectra were compared amongst each other. In several of the compounds there was a correlation between the UV-Vis and voltage output in each solvent. As seen in figure 18, homosalate had the highest UV-Vis absorbance in t-butanol, then in ethanol, and lastly in acetonitrile. This is also the case when looking at the voltage output; homosalate in t-butanol had the highest voltage, followed by ethanol, and acetonitrile. The same connection can be found between the data collected for oxybenzone. As seen in the UV-Vis data in figure 20, oxybenzone had the highest absorbance in acetonitrile, then ethanol, and lastly t-butanol which links to the voltage output in figure 21. In octocrylene, the link between UV-Vis and voltage is also there however, in its respective order with ethanol being the highest, then acetonitrile, and t-butanol last. When comparing the UV-Vis to the voltage output for octisalate a similar trend can be seen with acetonitrile, then ethanol, and t-butanol last as seen in figure 25. However, these trends are not as distinct as the rest of them, as in some areas in voltage there is a different order.

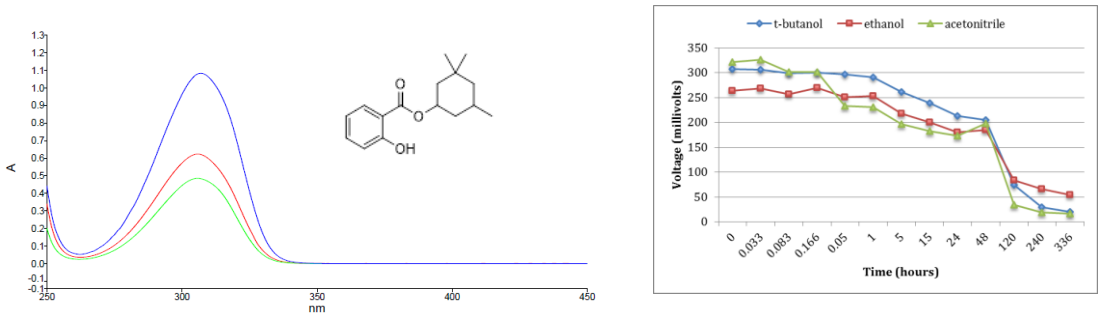

Figure 18 & 19: UV-Vis spectra and cell performance of Homosalate

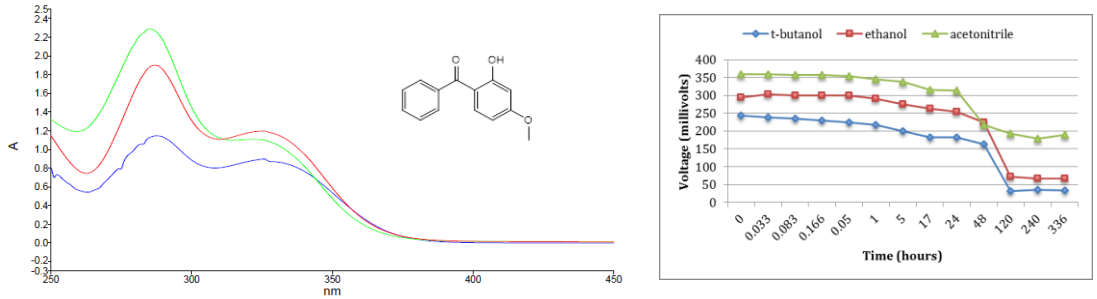

Figure 20 & 21: UV-Vis spectra and cell performance of Oxybenzone

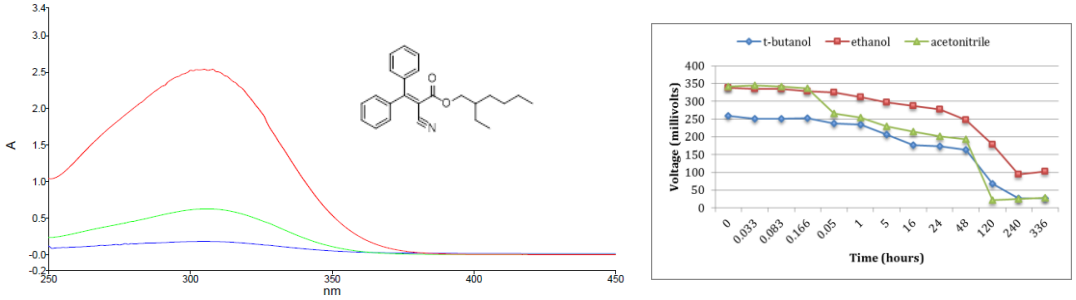

Figure 22 & 23: UV-Vis spectra and cell performance of Octocrylene

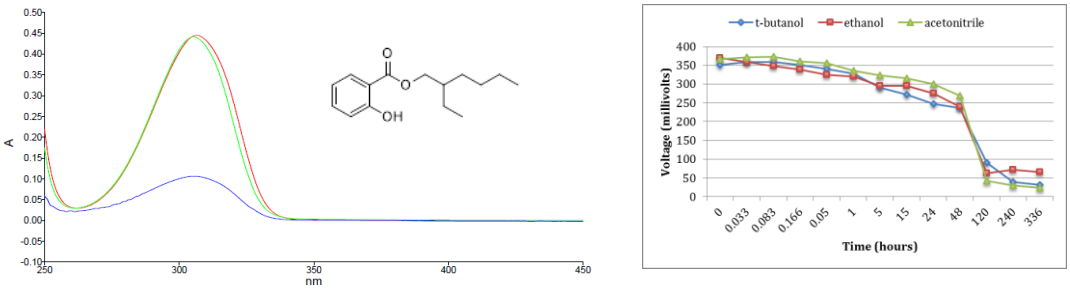

Figure 24 & 25: UV-Vis spectra and cell performance of Octisalate

Avobenzone in, figure 26, and compound B, in figure 28, were different than the other compounds. Both of these showed an opposite trend in voltage and UV-Vis. In UV-Vis they showed that acetonitrile would have the highest absorbance, followed by t-butanol, and lastly ethanol.

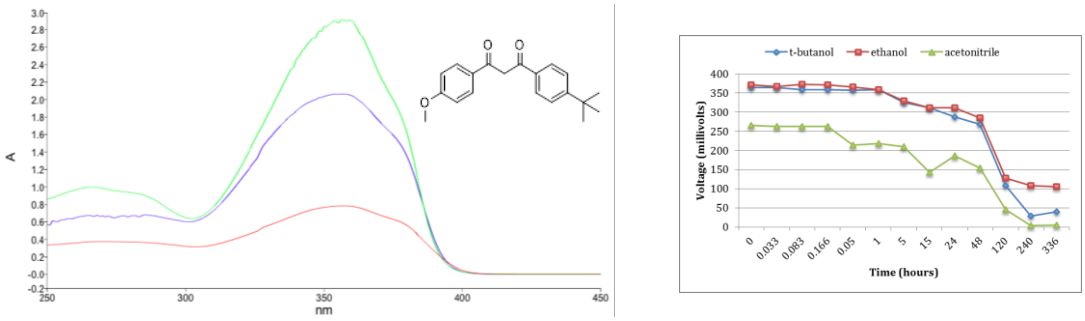

Figure 26 & 27: UV-Vis spectra and cell performance of Avobenzone

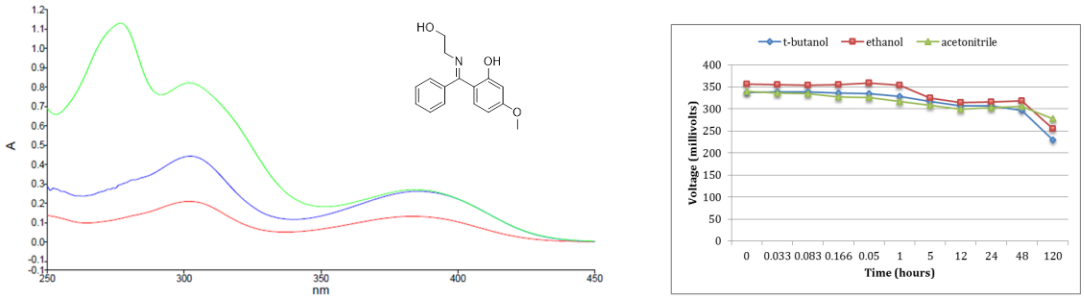

Figure 28 & 29: UV-Vis spectra and cell performance of Compound B

These trends were the exact opposite for in the voltage output for both the compounds. While the exact effect of these is unknown, it can be assumed that avobenzone's change in absorbance compared to voltage was due to its photoenolization. It is the only compound containing two carbonyl groups. Another reason why avobenzone may not have had the same correlation is because at certain concentrations it was not completely soluble in some solvents.

4.3 Cell Performance

The main data output was the measurement of voltage of each individual cell over time. Voltage output for each component is shown together in corresponding solvents over 336 hours. Main findings show consistent decreases in cell performance after 48 hours, and results are compared to that of baseline tests and new synthesized compounds.

4.3.1 Active Sunscreen Ingredients

To construct solar cells with each sensitizer, 0.05 molar solutions were created in three different solvents: t-butanol, ethanol, and acetonitrile. As discussed in section 4.1.1, additions of more than 200 µL of sensitizers seemed to make no apparent difference to the binding of TiO_2. Therefore, in each trial performed, only 200 µL of each solution were pipetted onto the TiO_2 layer assuming it would reach its saturation point. To test the cell's performance, the voltage and current were taken under room and UV light. While not trends were found from the current of the of the cell, the voltage performances of the sunscreen organic compounds were compared to those originally done with the anthocyanin's from blueberry juice. The cells with blueberry juice started with at average voltage output of 336 mV and only had a 45% decrease over 120 hours (see appendix C- blueberry juice voltage graph).

The voltage outputs of the five organic compounds were compared in the three different solvents. As seen in figure 30, the compound that had the highest voltage output in t-butanol was avobenzone with an initial voltage of 365 mV. Octisalate also surpassed the initial voltage of blueberry juice with an initial voltage of 352 mV.

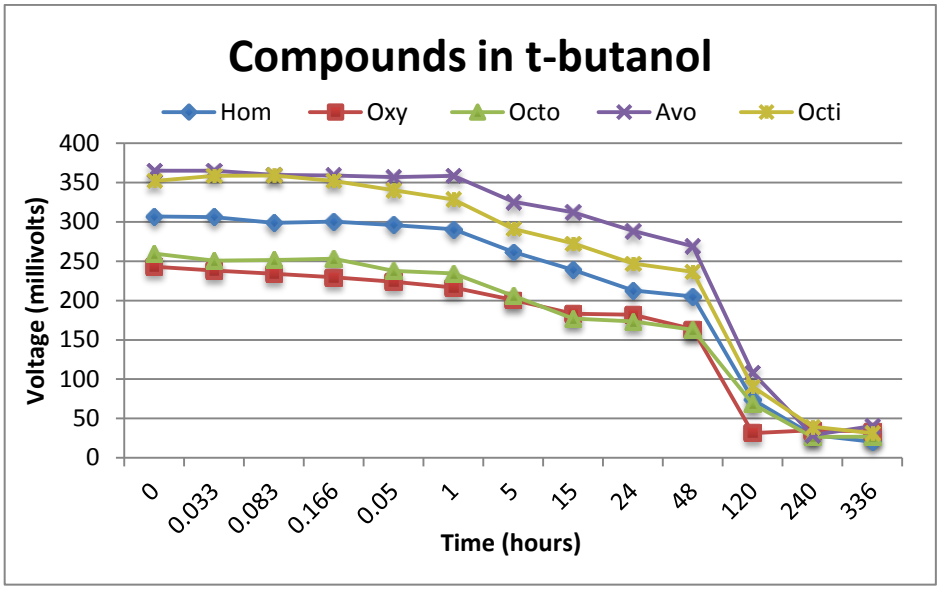

Figure 30: Voltage output of the five organic compounds in t-butanol

In ethanol there were three compounds that surpassed the initial voltage of blueberry juice avobenzone, octisalate, and octocrylene. These had 371 mV, 369.5 mV, and 337.5 mV respectively, as seen in figure 31.

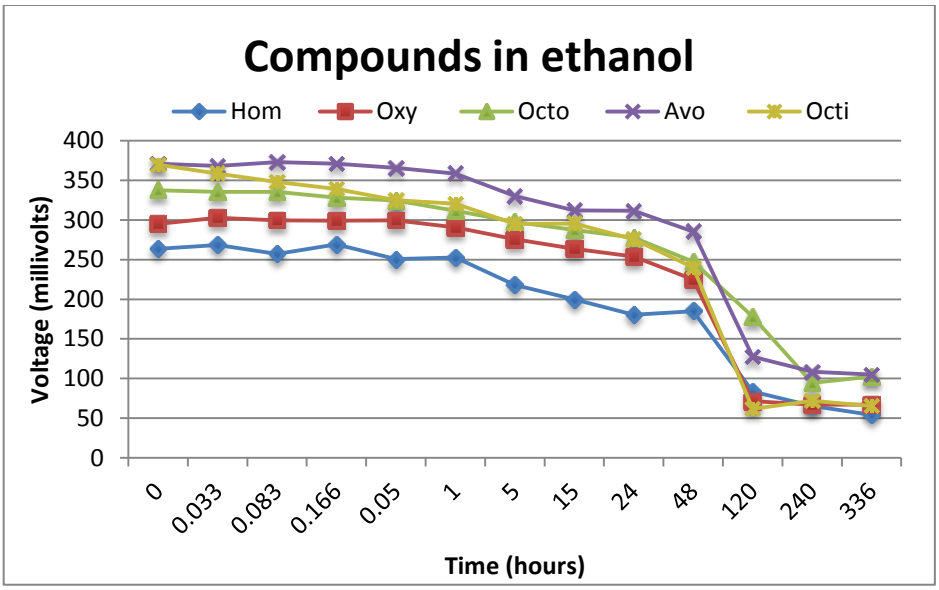

Figure 31: Voltage output of the five organic compounds in ethanol

In the acetonitrile solutions, the three compounds that surpassed the blueberry juice voltage output were octisalate, oxybenzone, and octocrylene with 366 mV, 358.2 mV, and 341.2 mV respectively as seen in figure 32.

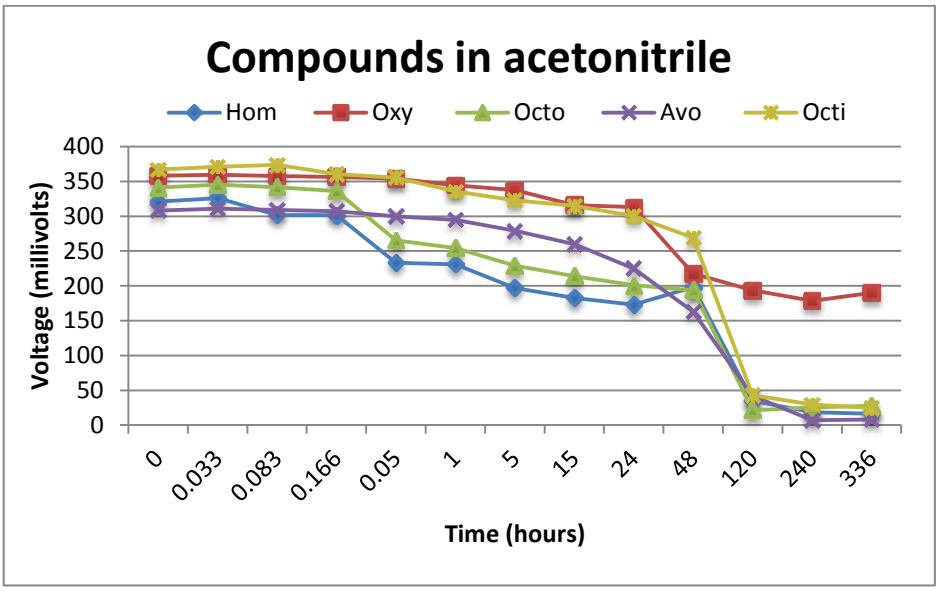

Figure 32: Voltage output of the five organic compounds in acetonitrile

One important factor that had to be taken into consideration was the percent decrease over time of the voltage output of each cell. Blueberry juice only had a 45% decrease over 120

hours, which is significantly lower than most of the compounds in all solvents. As seen in table 1, the 120 hours percent decrease for most compounds was in the 60% to 90% range. The only two exceptions were oxybenzone in acetonitrile and octocrylene in ethanol, which were in the 40% range. Since most of the decrease is between 48 and 120 hours, this percent decrease was also calculated. Table 2 shows the change most cells show during these time points. Once again, the exceptions were oxybenzone in acetonitrile, which only had an 11% decrease, and octocrylene in ethanol with a 28% decrease. When looking at the overall percent decrease (0-336 hours) in table 3, only oxybenzone in acetonitrile had a much lower percent decrease at 46.9%.

	t-butanol	ethanol	acetonitrile
Octisalate	74.2	83.2	88.2
Homosalate	75.8	68.3	89.2
Oxybenzone	87.0	75.7	45.9
Octocrylene	73.6	47.2	93.6
Avobenzone	70.4	65.6	86.3

Table 1: Percent decrease from 0-120 hours

	t-butanol	ethanol	acetonitrile
Octisalate	61.7	74.1	84.0
Homosalate	63.9	54.8	82.5
Oxybenzone	80.7	68.2	11.0
Octocrylene	57.9	28.0	88.9
Avobenzone	59.8	55.3	74.2

Table 2: Percent decrease from 48-120 hours

	t-butanol	ethanol	acetonitrile
Octisalate	91.0	82.2	93.3
Homosalate	93.3	79.5	94.9
Oxybenzone	86.2	77.2	46.9
Octocrylene	89.5	69.6	91.7
Avobenzone	88.9	71.6	97.4

Table 3: Percent decrease from 0-336 hours

In order to further analyze the effects that organic compounds could have on solar cells, different combinations were tested. The combinations were chosen by selecting two compounds, of which one was a stabilizer, which both had high cell performance in the same solvent.

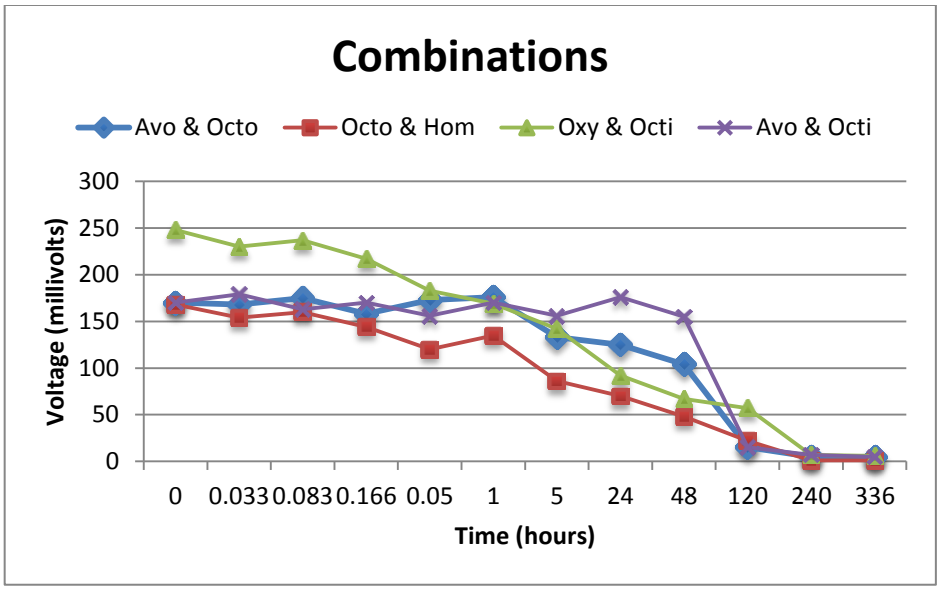

Figure 33: Cell performance of compound combinations: Avobenzone & Octocrylene in ethanol, Octisalate & Homosalate in ethanol, Oxybenzone & Octisalate in acetonitrile, and Avobenzone & Octisalate in ethanol

Figure 33 shows that the combinations attempted did not have a high voltage output; however, it could be inferred that the stability of the compounds was increased as some of them had a steadier slope over time; in particular, the combinations of oxybenzone & octisalate, and octocrylene & homosalate.

4.3.2 Synthetic Changes

Synthetic functional changes were made to oxybenzone. Compound A has a methyl amine group while compound B has an ethanolamine addition. Compound C, a salen ligand, was not investigated further due to insolubility. Both imine transformations showed a shift in UV-visible spectra. They resulted in increased voltage stability over time compared to their oxybenzone starting material.

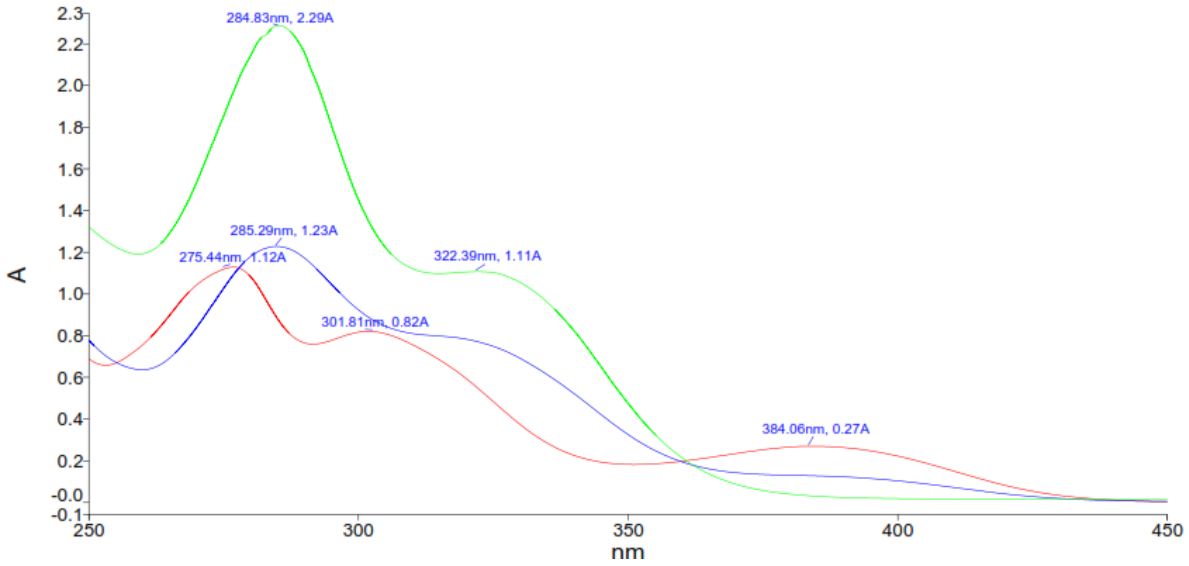

Figure 34: UV-Vis spectra of Oxybenzone, Compound A, and Compound B

In acetonitrile, there was a clear shift in UV-Vis spectra for the two analyzed compounds. There was a decrease in the absorbance of compounds A and B; however max values were shifted for each.

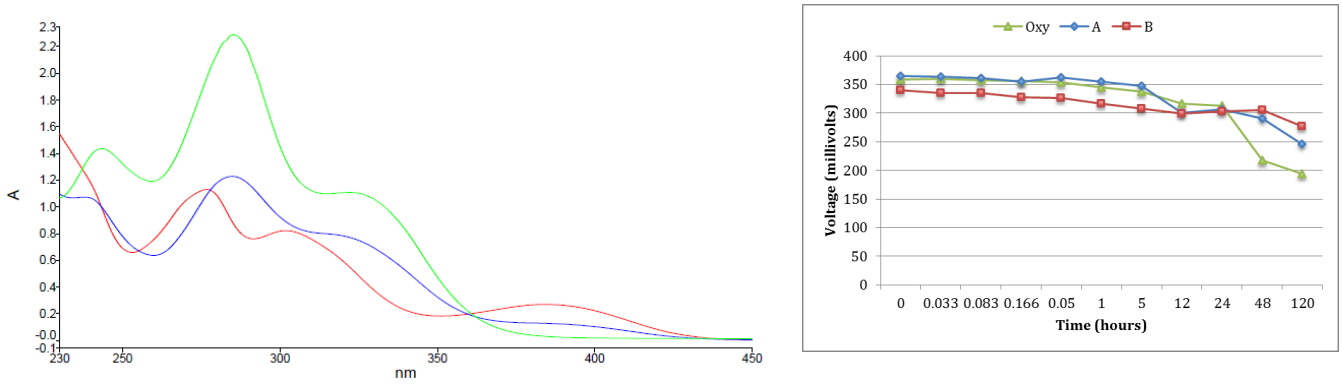

Figure 35: UV-Vis spectra vs. cell performance over 120 hours

Compared cell performance shows that initial voltage output is extremely consistent. Compounds A and B both showed increased stability after 48 hours.

4.3.3 Cell performance of Compound B

The cell performance of compound B was tested in all three solvents, just as the sunscreen organic ingredients were tested. The compound in the ethanol solution showed to have

a higher voltage at 356 mV, followed by 340 mV in acetonitrile, and 337.5 mV in t-butanol as seen in figure 36.

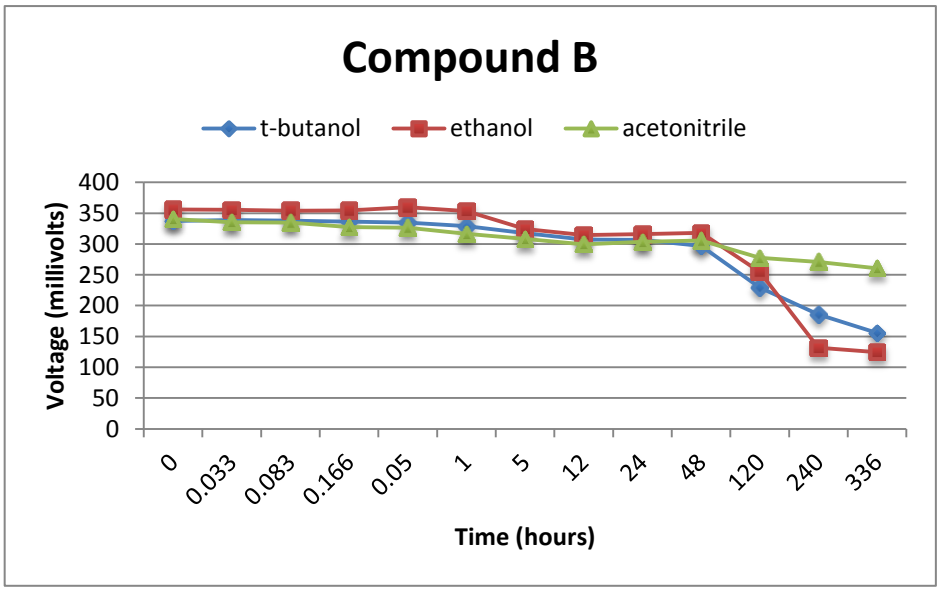

Figure 36: Cell performance of Compound B

	t-butanol	ethanol	acetonitrile
0-120 hours	32	28.3	18.5
48-120 hours	22.7	19.8	9.16
0-336 hours	53.9	65.0	23.4

Table 4: Percent decrease over time of Compound B

Even though a higher voltage was seen in the ethanol solution, all solutions had a much steadier decrease than the organic sunscreen ingredients over time. As can be seen in table 4, while ethanol solution showed the highest voltage output, the acetonitrile solution showed the least percent decrease over time.

5 Conclusion and Recommendations

The five major active ingredients in sunscreen, oxybenzone, avobenzone, octocrylene, octisalate, and homosalate, have shown that they have potential as light absorbing components for hybrid dye-sensitized solar cells. It was found that in a closed system their voltage output and absorbing ability remained stable far longer than the normal duration for sunscreen efficiency, suggesting that the closed system may decrease the rate of degradation.

Cells did not function properly if not saturated with molecules of the light absorbing component and it was found through IR that 200 µL of 0.05M solutions of each compound would properly coat the cell. Synthetic functional changes to oxybenzone in which an imine was added showed increased stability after 48 hours and, in the case of compound A, slightly higher cell potentials.

Multiple tests showed that solvent consideration is an integral part of hybrid dye-sensitized solar cells. Increased absorption in UV spectroscopy showed that UV absorbance was directly related to voltage output of cells with the corresponding absorbing component. Most compounds showed consistent stability for 48 hours, thereafter decreasing at the same rate. The compounds showed comparable results to that of a baseline test using blueberry juice, which contains known dyes called anthocyanins.

Results suggest that these active ingredients could be potential replacements for current sensitizers, and that additional synthetic functional changes as well as solvent optimization could continue to improve cell potential and long term stability.

References

Burton, T., Jenkins, N., Sharpe, D., & Bossanyi, E. (2011). *Wind energy handbook*: John Wiley & Sons.

Diffey, B. L., Tanner, P. R., Matts, P. J., & Nash, J. F. (2000). In vitro assessment of the broad-spectrum ultraviolet protection of sunscreen products. *Journal of the American Academy of Dermatology, 43*(6), 1024-1035.

Dincer, I. (2000). Renewable energy and sustainable development: a crucial review. *Renewable and Sustainable Energy Reviews, 4*(2), 157-175.

Foster, R., Ghassemi, M., & Cota, A. (2009). *Solar energy: renewable energy and the environment*: CRC Press.

Grätzel, M. (2003). Dye-sensitized solar cells. *Journal of Photochemistry and Photobiology C: Photochemistry Reviews, 4*(2), 145-153.

Hagfeldt, A., Boschloo, G., Sun, L., Kloo, L., & Pettersson, H. (2010). Dye-sensitized solar cells. *Chemical reviews, 110*(11), 6595-6663.

Hardin, B. E., Snaith, H. J., & McGehee, M. D. (2012). The renaissance of dye-sensitized solar cells. *Nat Photon, 6*(3), 162-169.

Johansson, T. B., & Burnham, L. (1993). *Renewable energy: sources for fuels and electricity*: Island Press.

King, D. L., Kratochvil, J. A., & Boyson, W. E. (1997). *Measuring solar spectral and angle-of-incidence effects on photovoltaic modules and solar irradiance sensors.* Paper presented at the Photovoltaic Specialists Conference, 1997., Conference Record of the Twenty-Sixth IEEE.

Lee, S., Speight, J. G., & Loyalka, S. K. (2007). *Handbook of alternative fuel technologies*: crc Press.

Mishra, A., Fischer, M. K., & Bäuerle, P. (2009). Metal-free organic dyes for dye-sensitized solar cells: From structure: Property relationships to design rules. *Angewandte Chemie International Edition, 48*(14), 2474-2499.

Nathan, S. L., Crabtree, G., Nozik, A. J., Wasielewski, M. R., & Alivisatos, P. (2005). *Basic research needs for solar energy utilization*.

Nault, R. M. (2005). Report on the basic energy sciences workshop on solar energy utilization. *Argonne National Laboratory USA*.

Nazeeruddin, M. K., Baranoff, E., & Grätzel, M. (2011). Dye-sensitized solar cells: a brief overview. *Solar Energy, 85*(6), 1172-1178.

O'Regan, B., & Gratzel, M. (1991). A low-cost, high-efficiency solar cell based on dye-sensitized colloidal TiO2 films. *Nature, 353*(6346), 737-740.

Routray, W., & Orsat, V. (2011). Blueberries and their anthocyanins: Factors affecting biosynthesis and properties. *Comprehensive Reviews in Food Science and Food Safety, 10*(6), 303-320.

Sambandan, D. R., & Ratner, D. (2011). Sunscreens: an overview and update. *Journal of the American Academy of Dermatology, 64*(4), 748-758.

Sariciftci, N. S., Smilowitz, L., Heeger, A. J., & Wudl, F. (2003). Semiconducting polymers (as donors) and buckminsterfullerene (as acceptor): photoinduced electron transfer and heterojunction devices. *Synthetic Metals, 59*(3), 333-352.

Saunders, B. R., & Turner, M. L. (2008). Nanoparticle-polymer photovoltaic cells. *Advances in Colloid and Interface Science, 138*(1), 1-23.

Shaheen, S. E., Ginley, D. S., & Jabbour, G. E. (2005). Organic-Based Photovoltaics: Toward Low-Cost Power Generation. *Materials Research Society Bulletin, 30,* 10-19.

Strümpel, C., McCann, M., Geaucarne, G., Arkhipov, V., Slaoui, A., Svrcek, V., . . . Tobias, I. (2006). Modifying the solar spectrum to enhance silicon solar cell efficiency - An overview of available materials. *Solar Energy Materials & Solar Cells, 91*(1), 238-249.

Stupp, S. I., Herman, D. J., Goldberger, J. E., Chao, S., & Martin, D. T. (2011). Orienting Periodic Organic-Inorganic Nanoscale Domains Through One-Step Electrodeposition. *ACS Nano, 5*(1), 565-573.

Sukhatme, K., & Sukhatme, S. P. (1996). *Solar energy: principles of thermal collection and storage*: Tata McGraw-Hill Education.

Weickert, J., Dunbar, R. B., Wiedemann, W., Hesse, H. C., & Schmidt-Mende, L. (2011). Nanostructured Organic and Hybrid Solar Cells. *Advanced Materials, 23*(16), 1810-1828.

Appendix A: IR

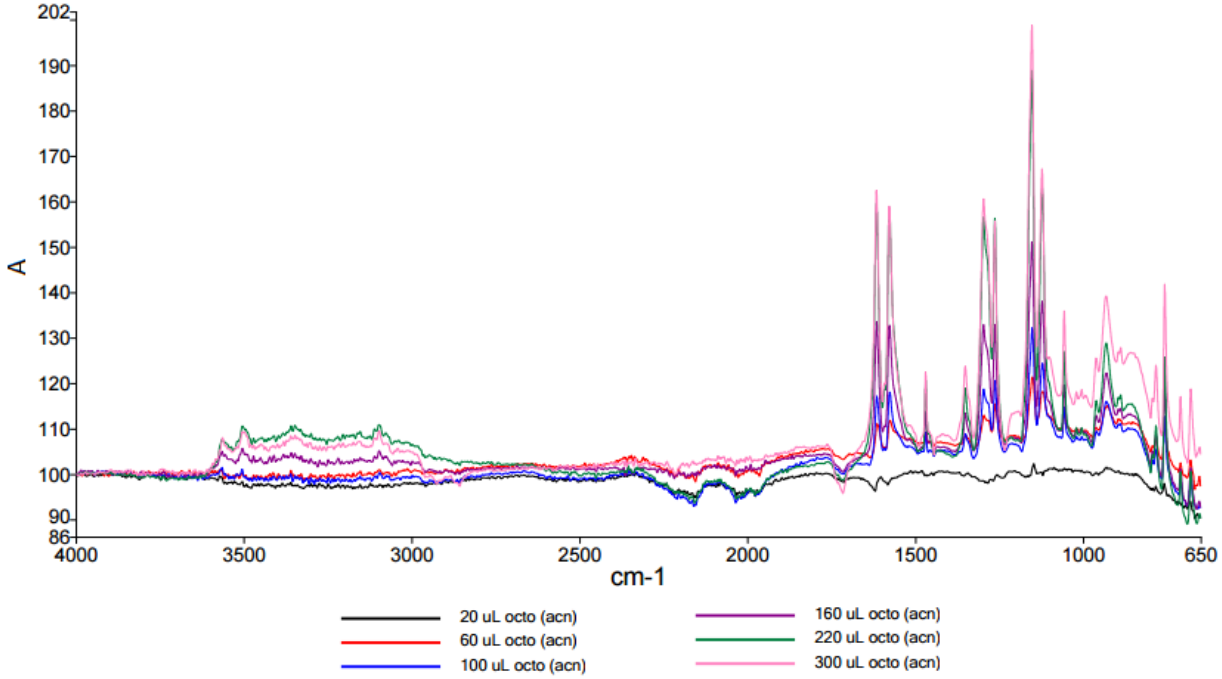

Absorbance of successive additions of octocrylene.

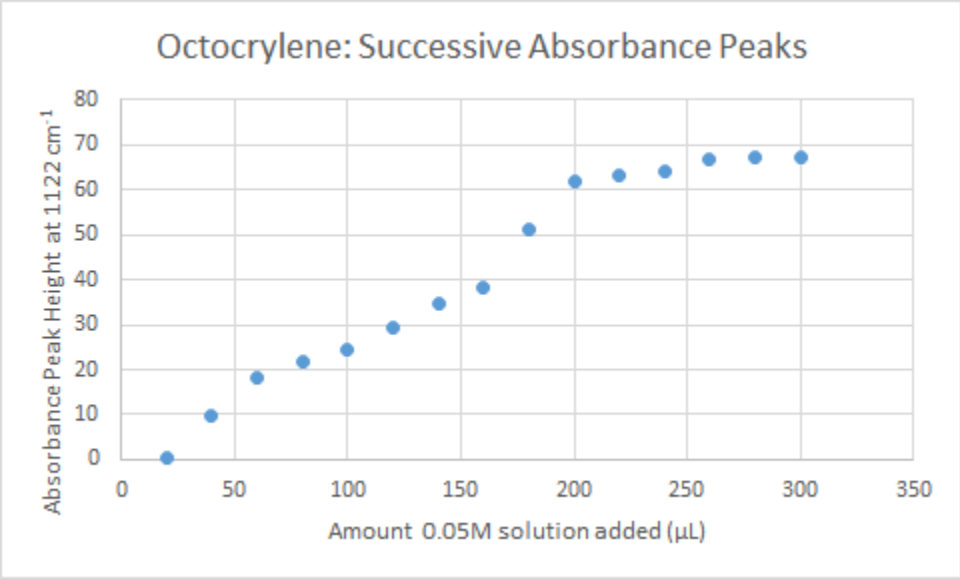

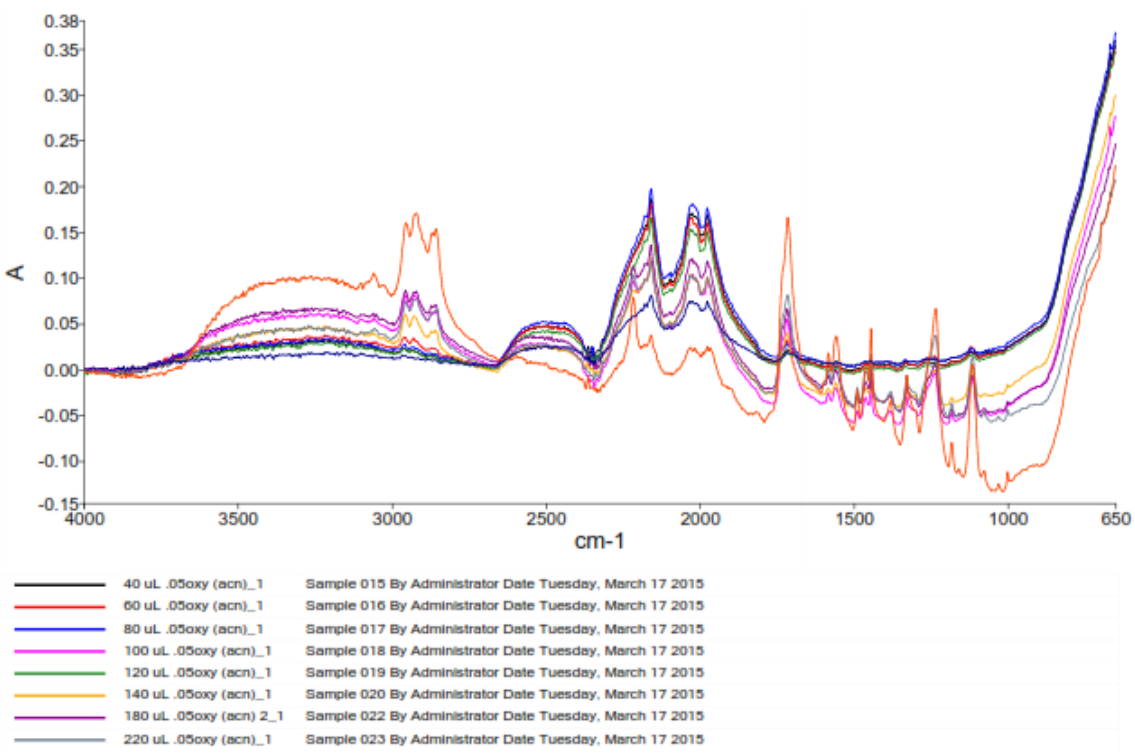

Absorbance of successive additions of oxybenzone.

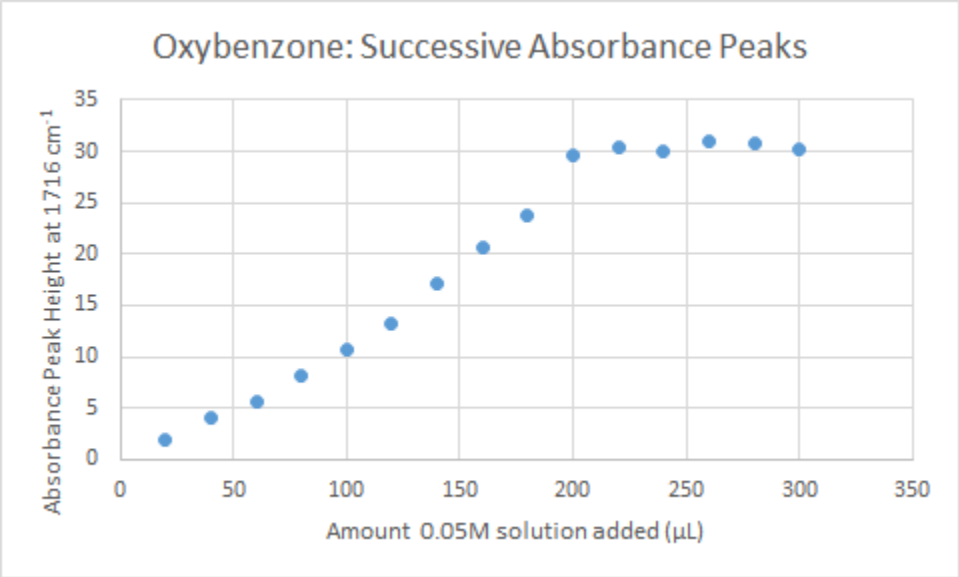

Appendix B: UV VIS Spectra

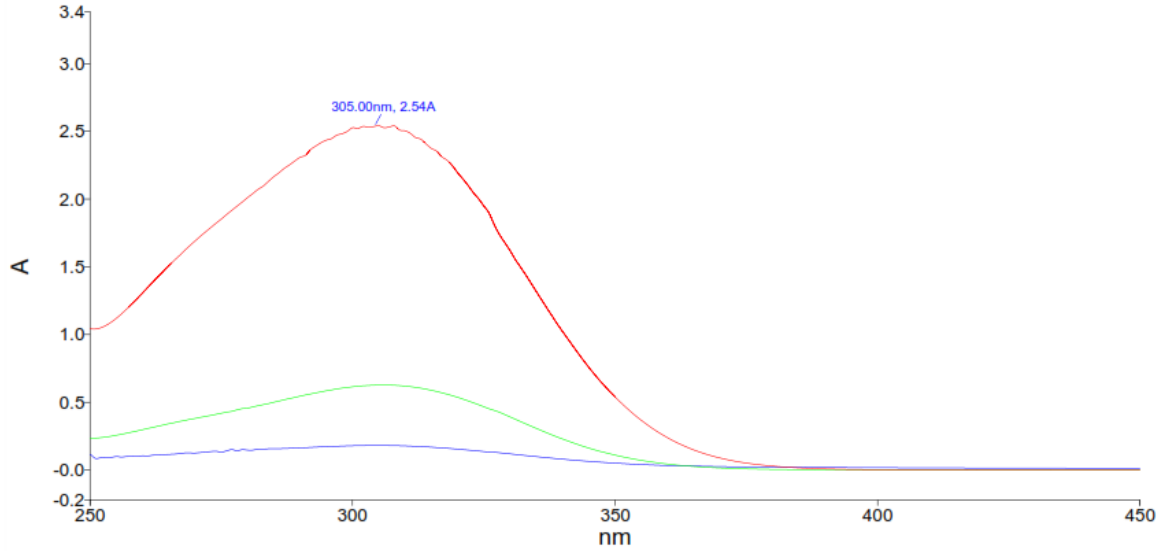

UV-Vis spectra of octocrylene in ethanol (red), acetonitrile (green), and t-butanol (blue).

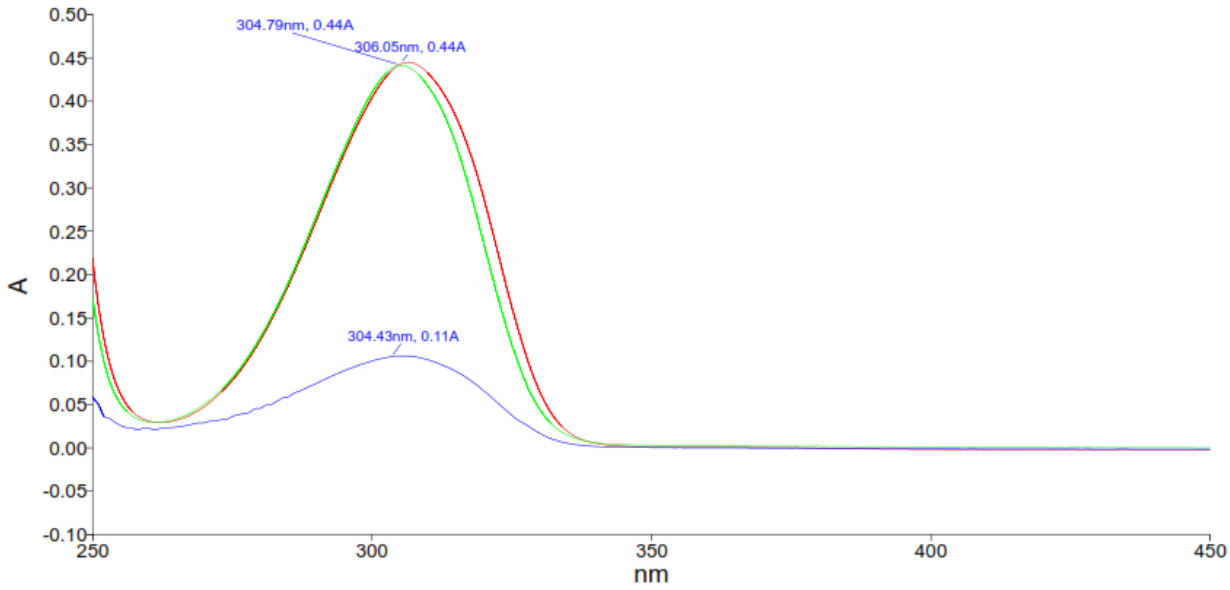

UV-Vis spectra of octisalate in ethanol (red), acetonitrile (green), and t-butanol (blue).

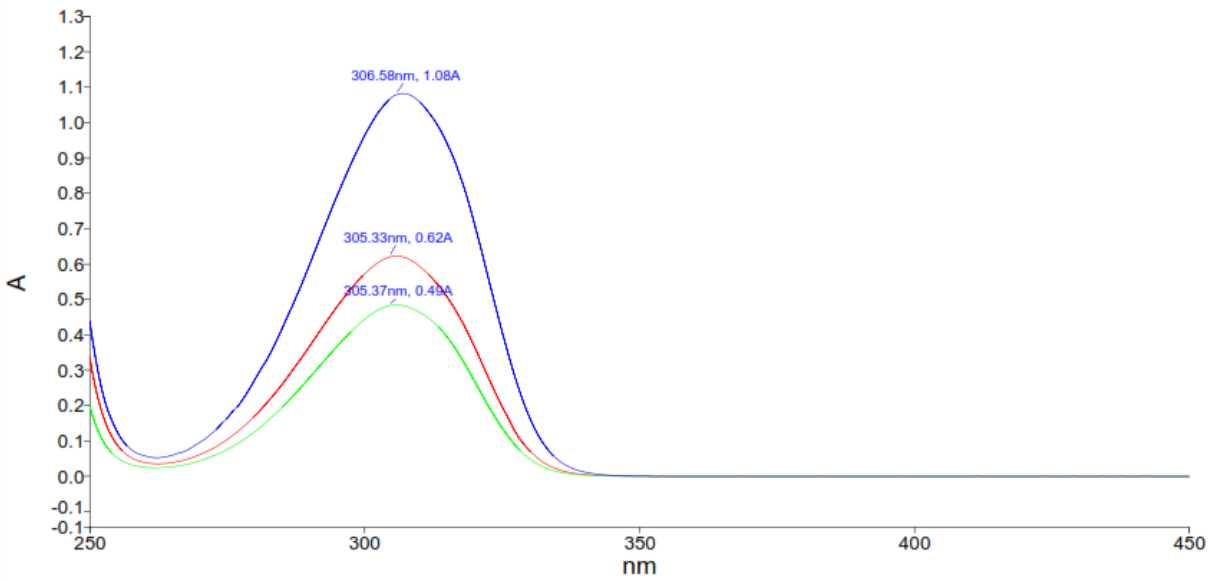

UV-Vis spectra of homosalate in t-butanol (blue), ethanol (red), and acetonitrile (green)

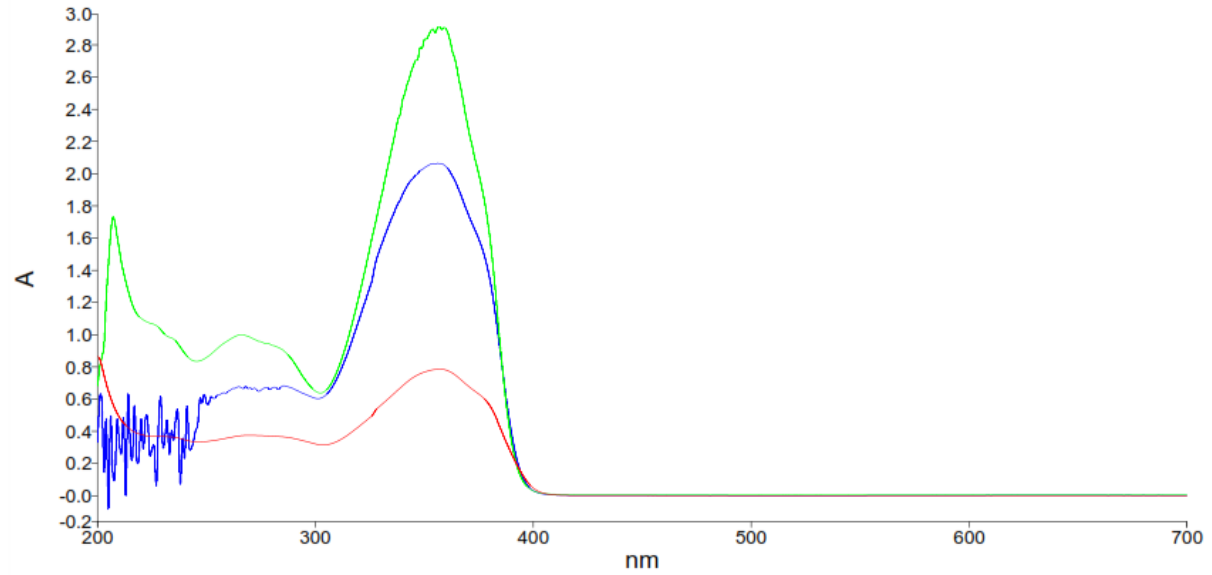

UV-Vis spectra of avobenzone in acetonitrile (green), t-butanol (blue) and ethanol (red)

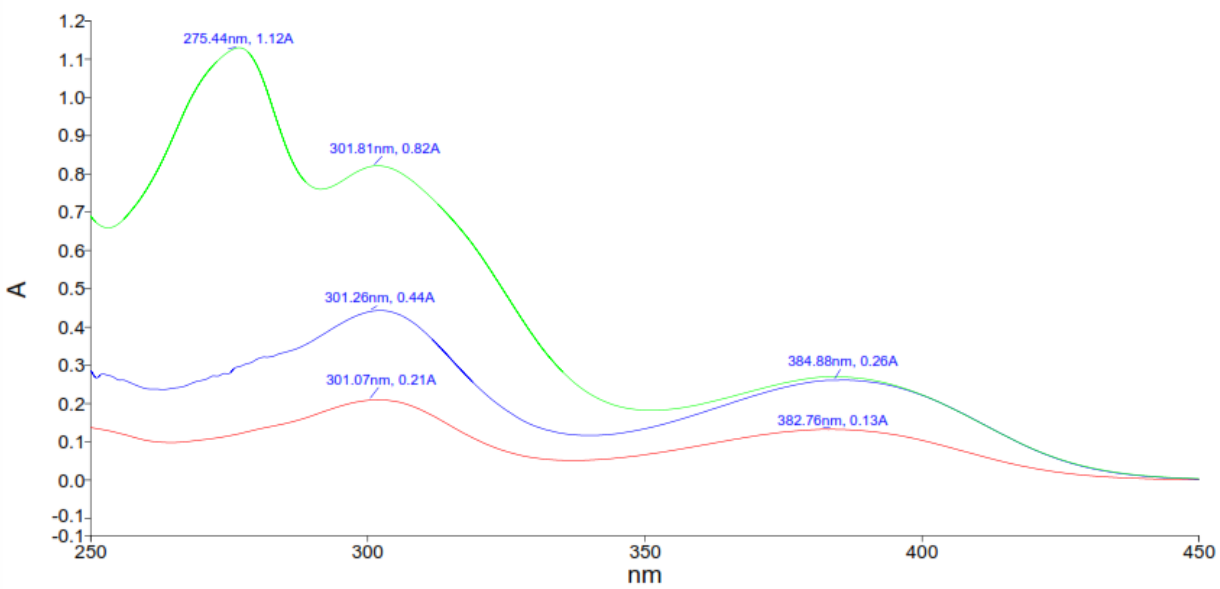

UV-Vis spectra of Compound B in ethanol (red), acetonitrile (green), and t-butanol (blue).

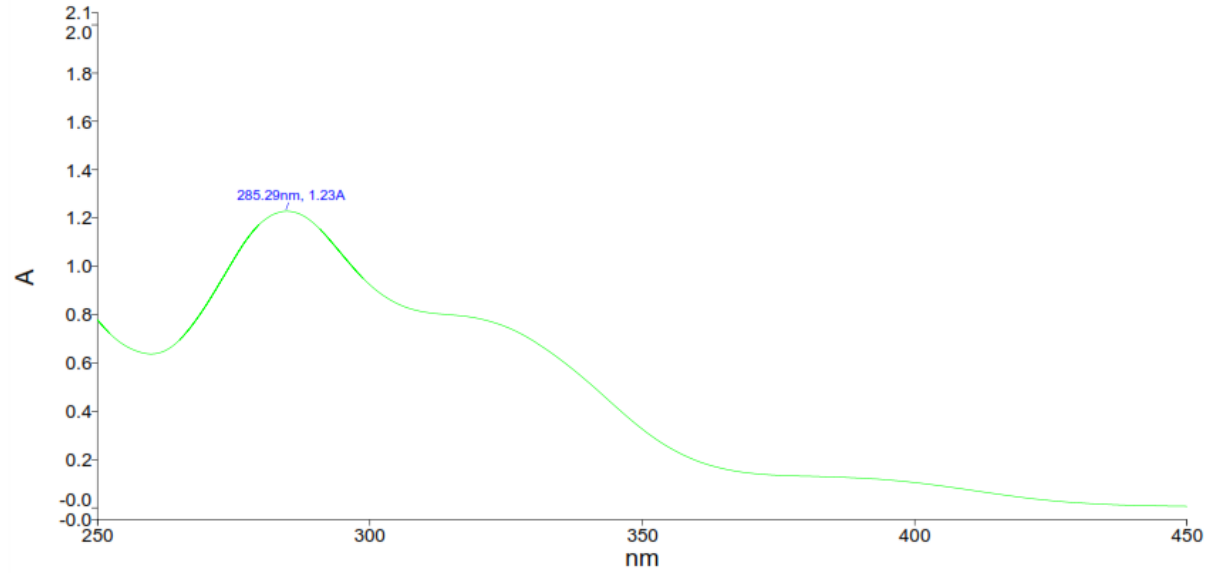

UV-Vis Spectra of Compound A in ethanol (red), acetonitrile (green), and t-butanol (blue).

Appendix C:

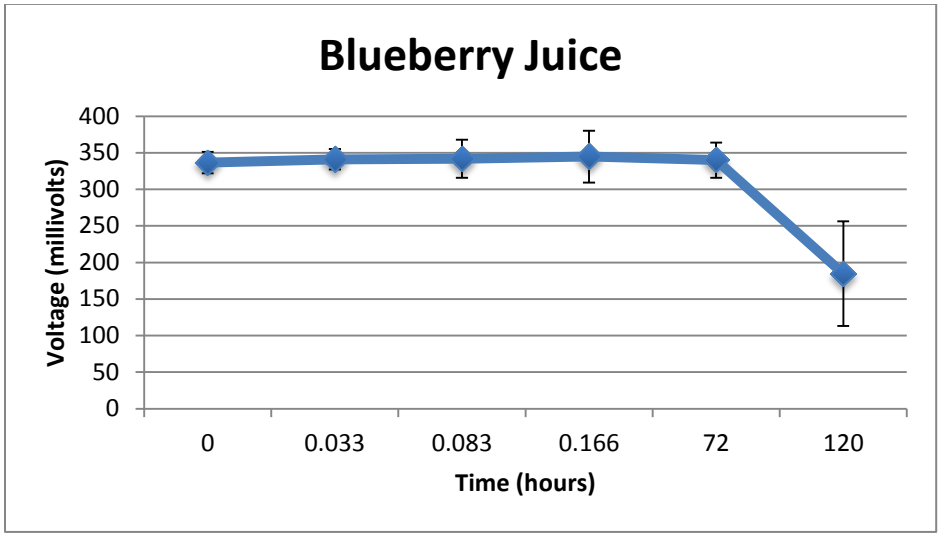
Blueberry Juice
Voltage (millivolts)
400
350
300
250
200
150
100
50
0
0
0.033
0.083
0.166
72
120
Time (hours)

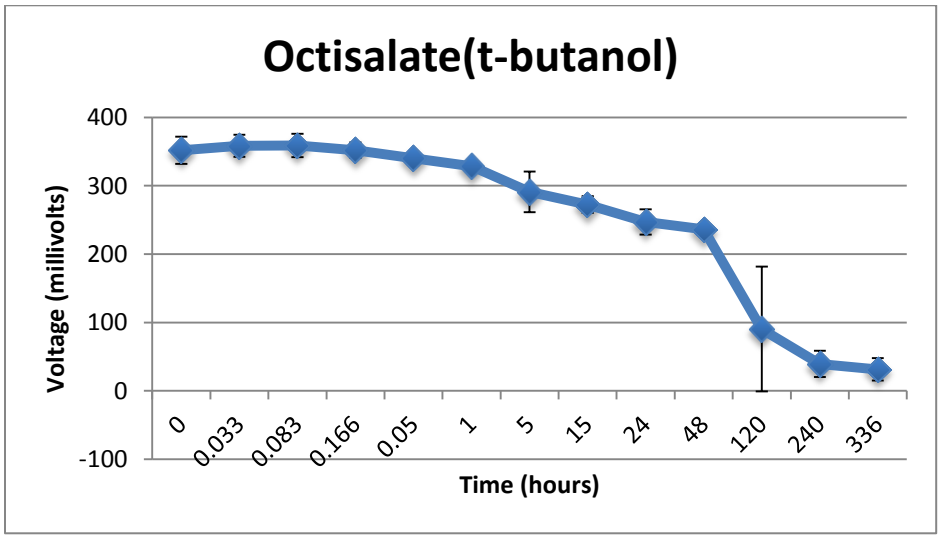
Octisalate(t-butanol)
Voltage (millivolts)
400
300
200
100
0
-100
0
0.033
0.083
0.166
0.05
1
5
15
24
48
120
240
336
Time (hours)

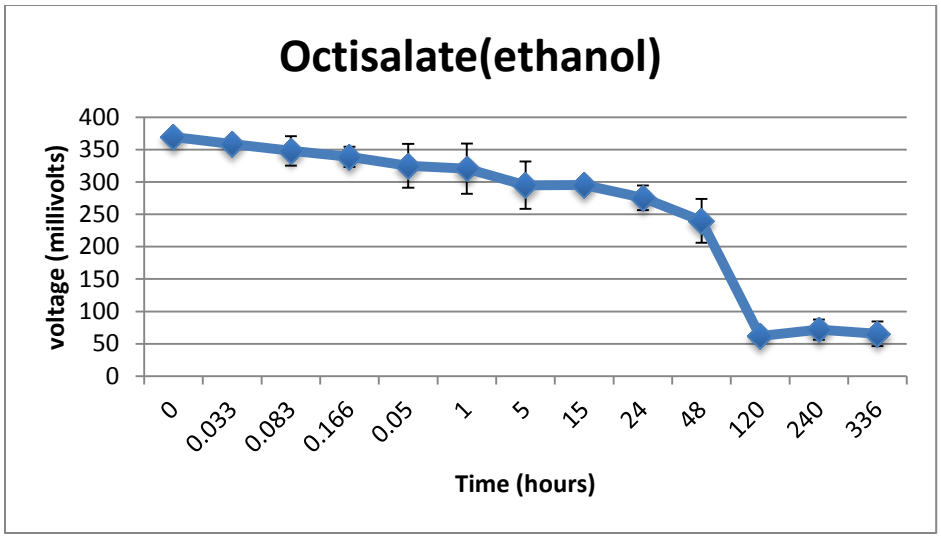
Octisalate(ethanol)
voltage (millivolts)
400
350
300
250
200
150
100
50
0
0
0.033
0.083
0.166
0.05
1
5
15
24
48
120
240
336
Time (hours)

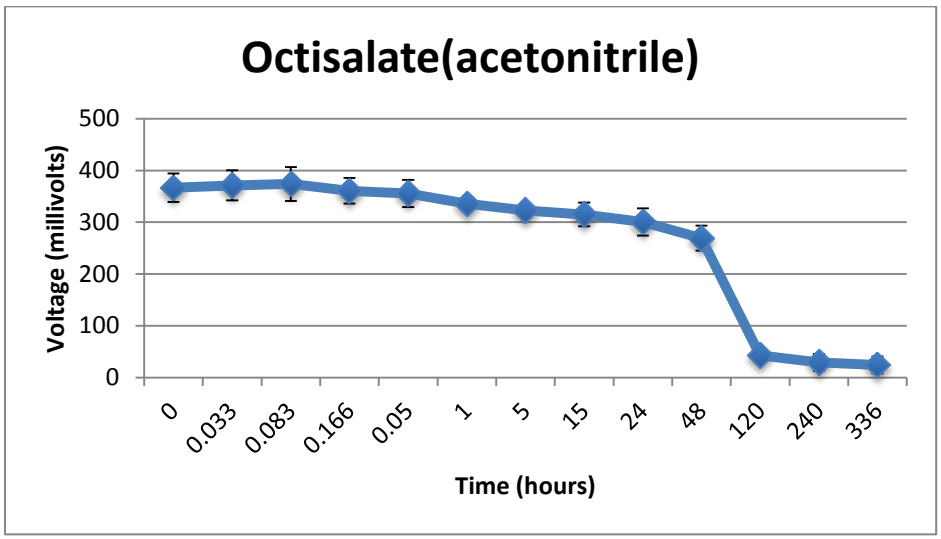
Octisalate(acetonitrile)
Voltage (millivolts)
500
400
300
200
100
0
0
0.033
0.083
0.166
0.05
1
5
15
24
48
120
240
336
Time (hours)

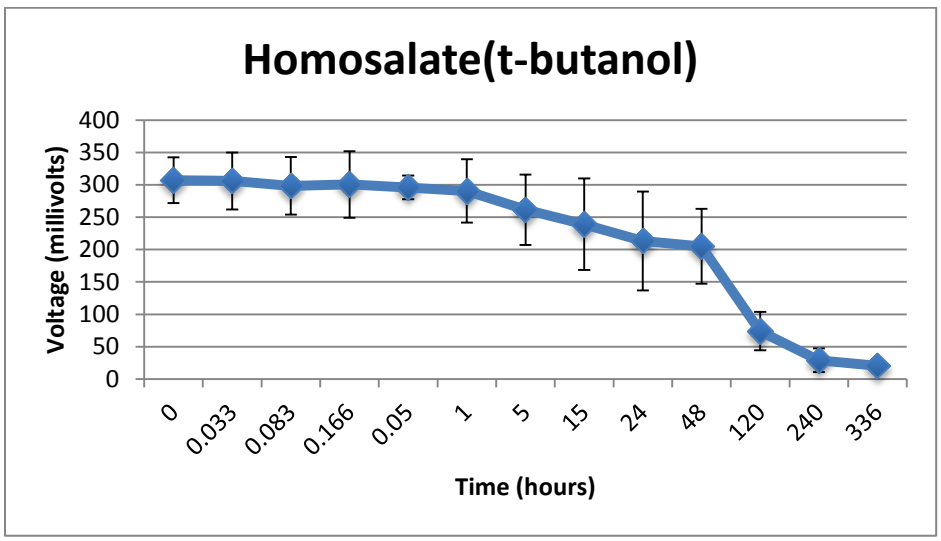
Homosalate(t-butanol)
Voltage (millivolts)
400
350
300
250
200
150
100
50
0
0
0.033
0.083
0.166
0.05
1
5
15
24
48
120
240
336
Time (hours)

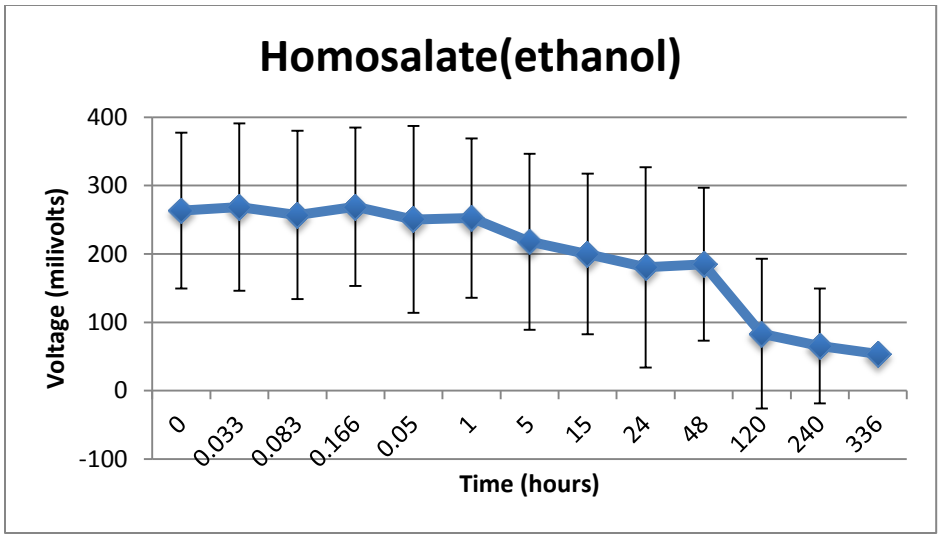
Homosalate(ethanol)
Voltage (milivolts)
400
300
200
100
0
-100
0
0.033
0.083
0.166
0.05
1
5
15
24
48
120
240
336
Time (hours)

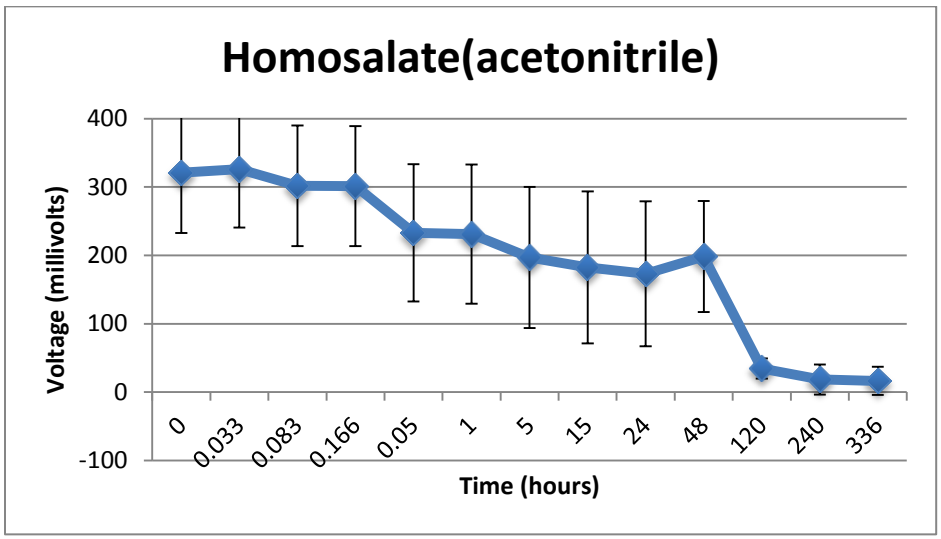
Homosalate(acetonitrile)
Voltage (millivolts)
400
300
200
100
0
-100
0
0.033
0.083
0.166
0.05
1
5
15
24
48
120
240
336
Time (hours)

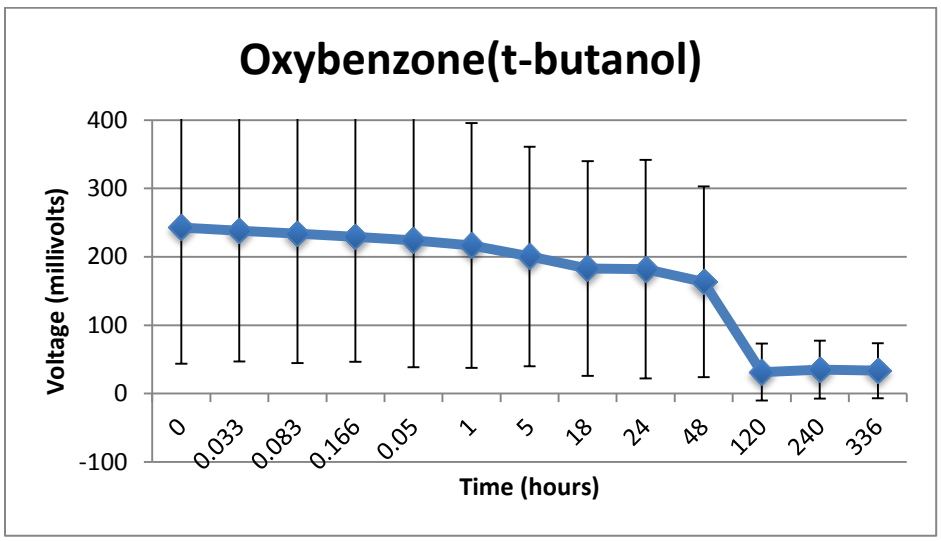
Oxybenzone(t-butanol)
Voltage (millivolts)
400
300
200
100
0
-100
0
0.033
0.083
0.166
0.05
1
5
18
24
48
120
240
336
Time (hours)

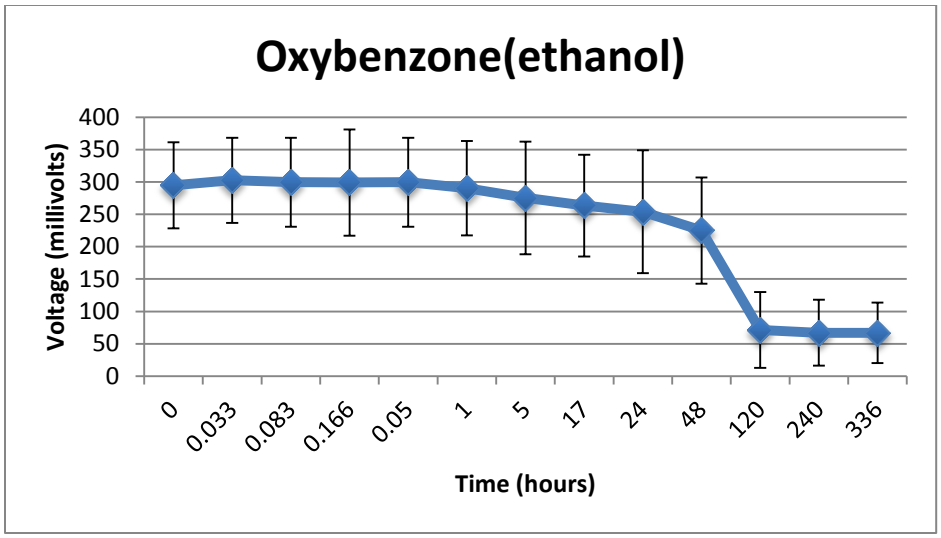
Oxybenzone(ethanol)
Voltage (millivolts)
400
350
300
250
200
150
100
50
0
0
0.033
0.083
0.166
0.05
1
5
17
24
48
120
240
336
Time (hours)

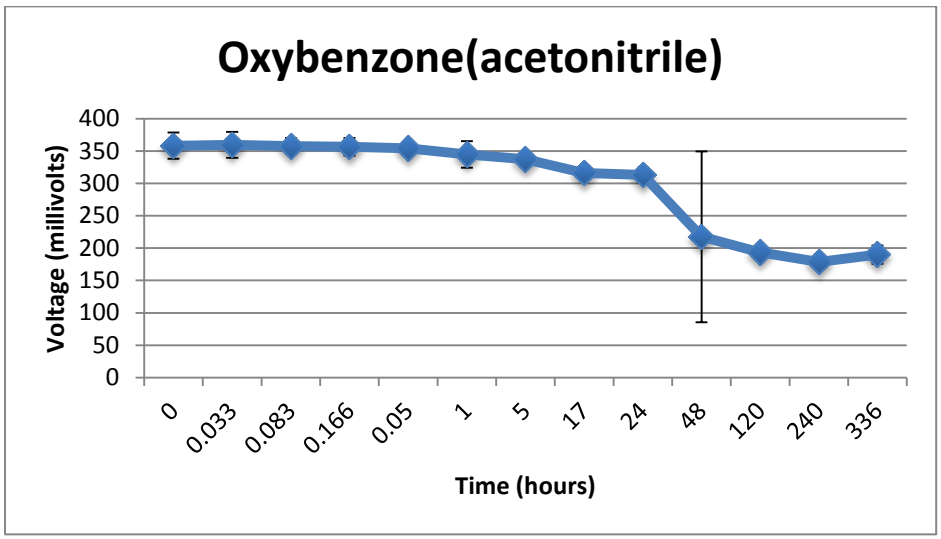
Oxybenzone(acetonitrile)
Voltage (millivolts)
400
350
300
250
200
150
100
50
0
0
0.033
0.083
0.166
0.05
1
5
17
24
48
120
240
336
Time (hours)

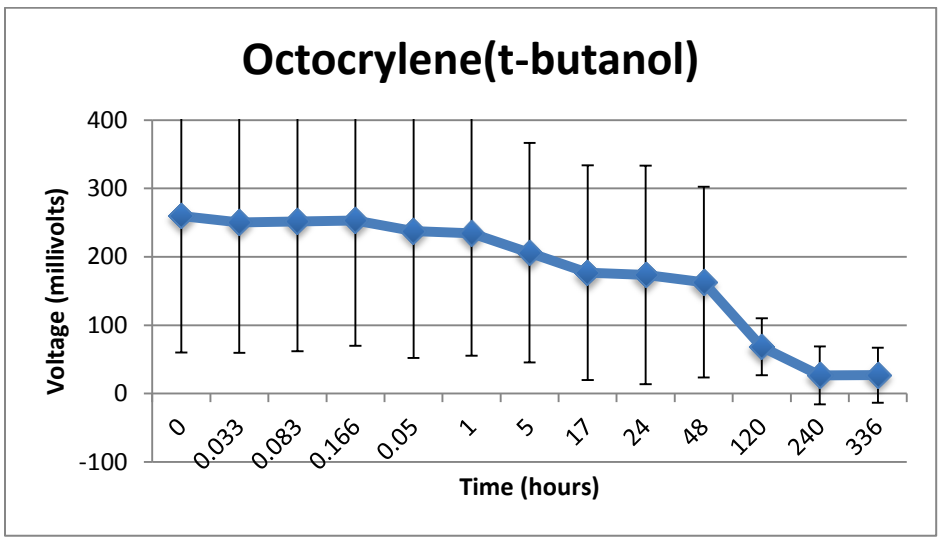
Octocrylene(t-butanol)
Voltage (millivolts)
400
300
200
100
0
-100
0
0.033
0.083
0.166
0.05
1
5
17
24
48
120
240
336
Time (hours)

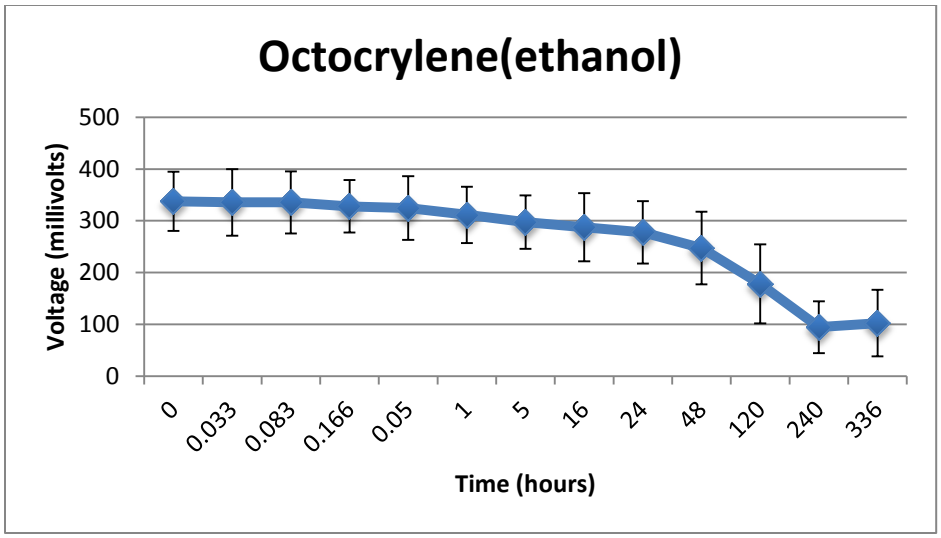
Octocrylene(ethanol)
Voltage (millivolts)
500
400
300
200
100
0
0
0.033
0.083
0.166
0.05
1
5
16
24
48
120
240
336
Time (hours)

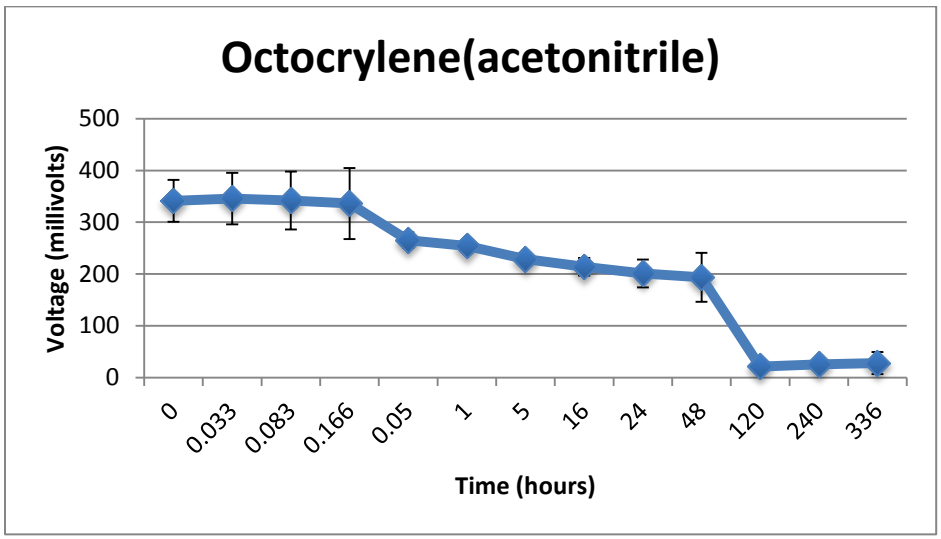
Octocrylene(acetonitrile)
Voltage (millivolts)
500
400
300
200
100
0
0
0.033
0.083
0.166
0.05
1
5
16
24
48
120
240
336
Time (hours)

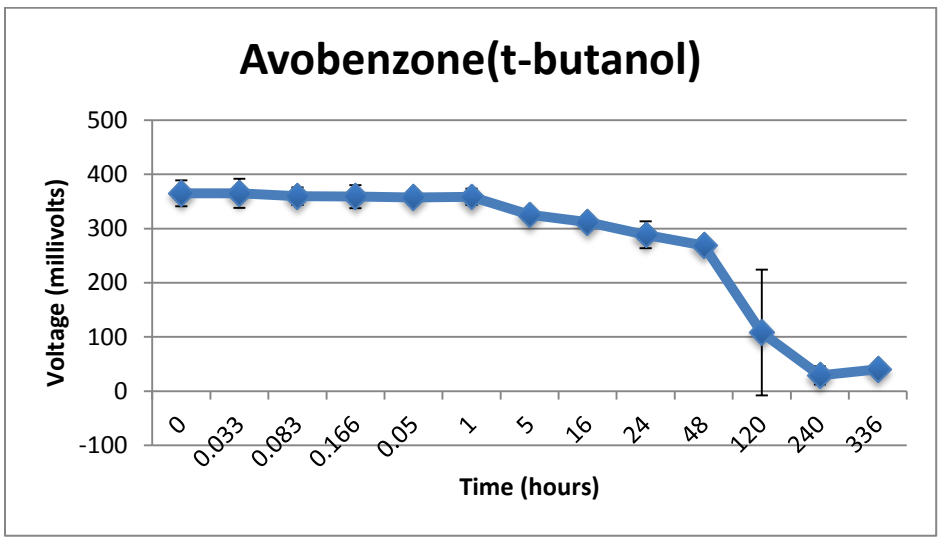
Avobenzone(t-butanol)
Voltage (millivolts)
500
400
300
200
100
0
-100
0
0.033
0.083
0.166
0.05
1
5
16
24
48
120
240
336
Time (hours)

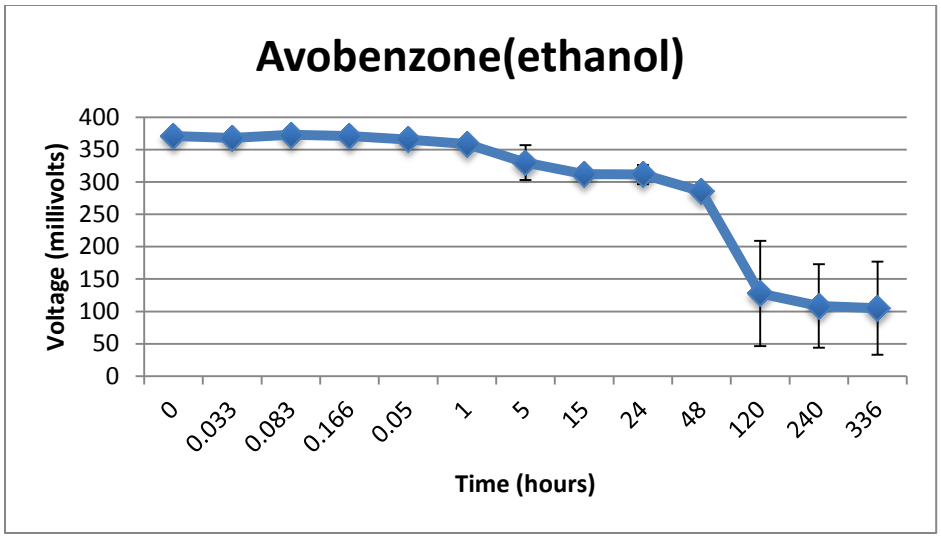
Avobenzone(ethanol)
Voltage (millivolts)
400
350
300
250
200
150
100
50
0
0
0.033
0.083
0.166
0.05
1
5
15
24
48
120
240
336
Time (hours)

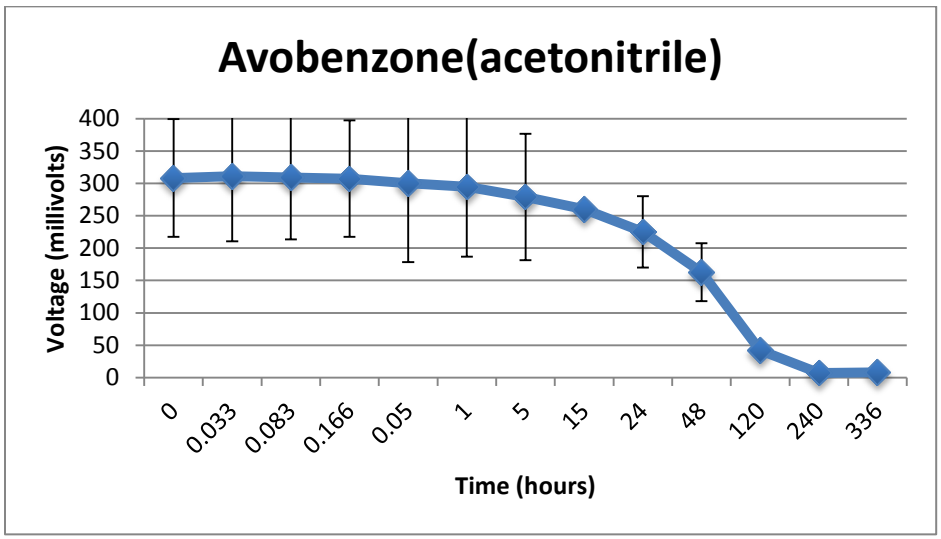
Avobenzone(acetonitrile)
Voltage (millivolts)
400
350
300
250
200
150
100
50
0
0
0.033
0.083
0.166
0.05
1
5
15
24
48
120
240
336
Time (hours)

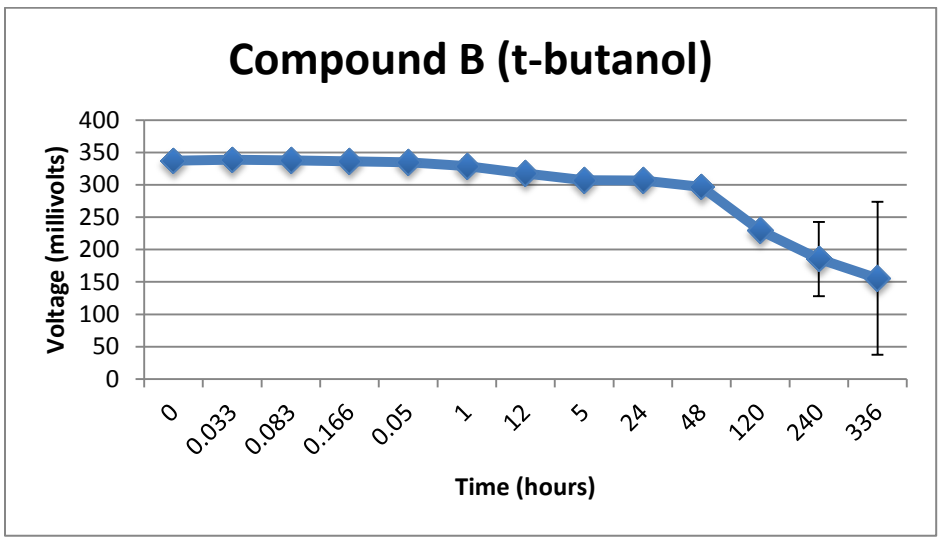
Compound B (t-butanol)
Voltage (millivolts)
400
350
300
250
200
150
100
50
0
0
0.033
0.083
0.166
0.05
1
12
5
24
48
120
240
336
Time (hours)

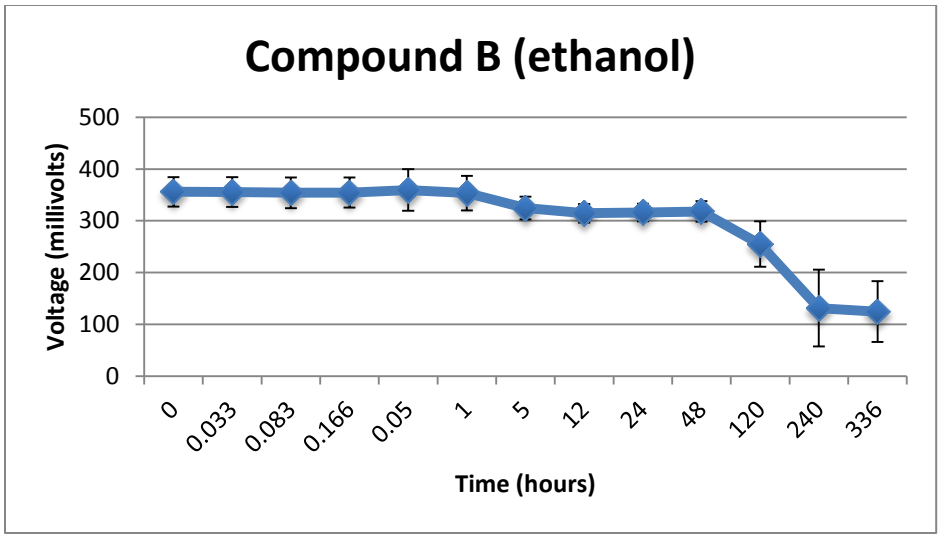
Compound B (ethanol)
Voltage (millivolts)
500
400
300
200
100
0
0
0.033
0.083
0.166
0.05
1
5
12
24
48
120
240
336
Time (hours)

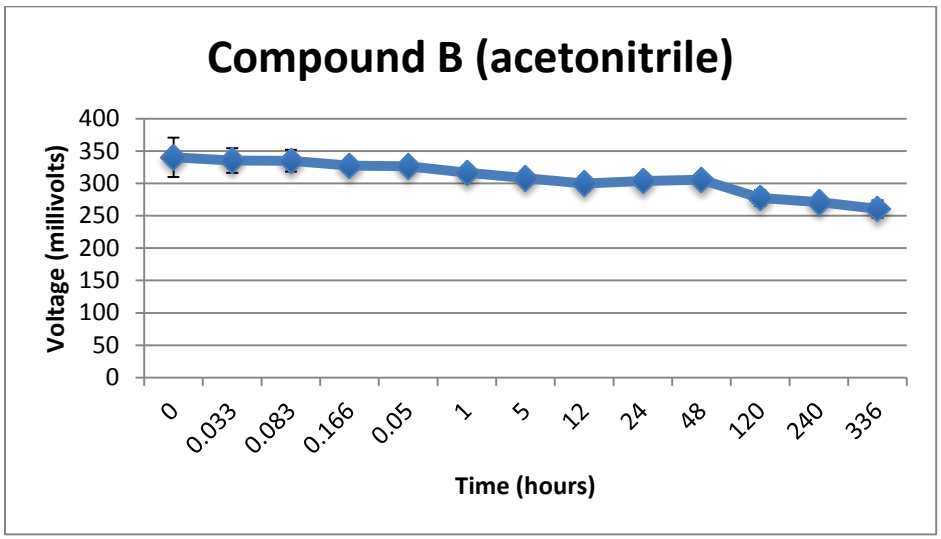
Compound B (acetonitrile)
Voltage (millivolts)
400
350
300
250
200
150
100
50
0
0
0.033
0.083
0.166
0.05
1
5
12
24
48
120
240
336
Time (hours)

Appendix D: Supplementary Material

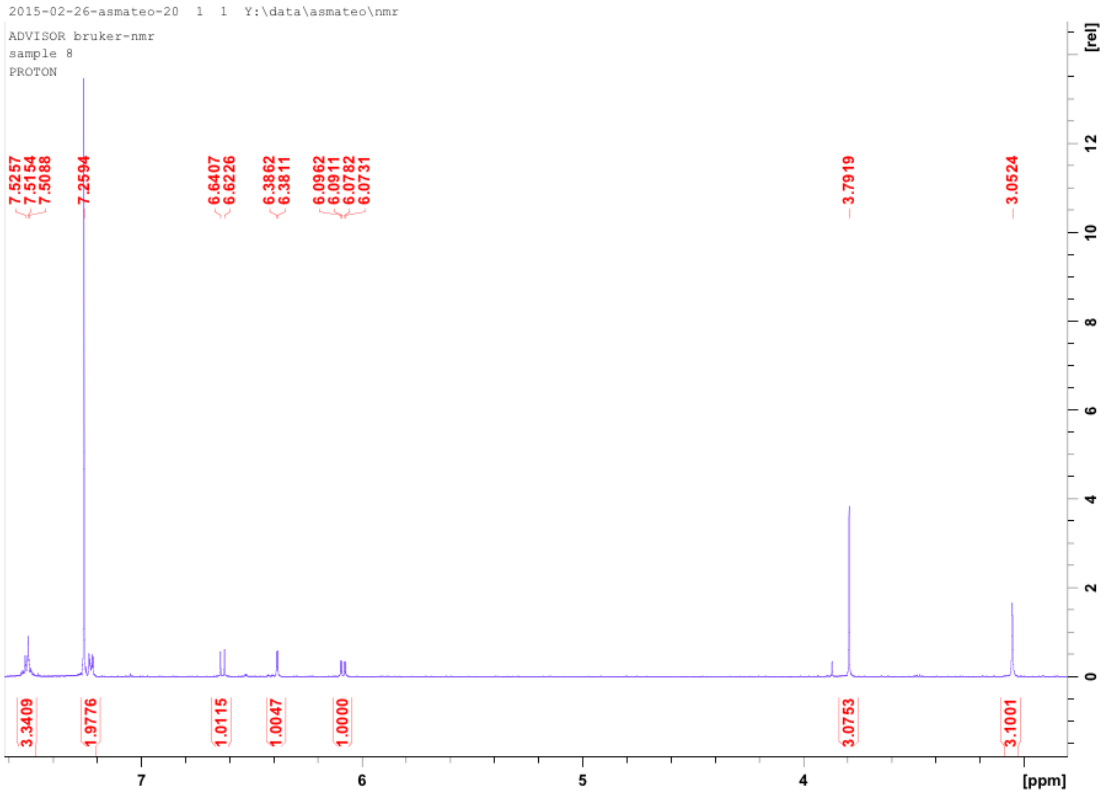

NMR of Compound A

```
Print of window 38: Current Chromatogram(s)
Data File  : C:\CHEM32\1\DATA\SEQUATIERI\DEFAULT_SERIES 2015-03-26 10-27-15\1EB-0201.D
Sample Name : SQ-8
======================================================================
Acq. Operator    : sequatieri                    Seq. Line :   2
Acq. Instrument : Instrument 1                   Location : P1-E-02
Injection Date  : 3/26/2015 10:42:54 AM             Inj :   1
                                                 Inj Volume : 2 µl
Acq. Method      : C:\Chem32\1\DATA\SEQUATIERI\DEFAULT_SERIES 2015-03-26 10-27-15\ACID_
                   GRAD_SERIES.M
Last changed     : 6/19/2014 11:31:36 AM by ABUTLER
Analysis Method : C:\CHEM32\1\DATA\SEQUATIERI\DEFAULT_SERIES 2015-03-26 10-27-15\1EB-
                   0201.D\DA.M (ACID_GRAD_SERIES.M)
Last changed     : 6/19/2014 11:31:36 AM by ABUTLER
Method Info      : Method: APB_ACID_GRAD_SERIES.M, multi-sample, 18 minutes run time/
                   sample
                   2uL injection with 10sec Needle Wash (flushport) for LC-MS, ESI+/-,
                   m/z 180-1200
                   Use with Sequence DEFAULT_SERIES.S, tune file: atunes_dual_fast.TUN
                   A1 H2O 0.1% FA, B1 95%ACN/5%H2O w0.1%FA,
                   0.3ml/Min gradient, 8 minutes, 30oC, Column 1
                   *For Use with ES Ind. Epic C18 MSO, 2.3u, 150A, 5cmx2.1mm column, S/
                   N: 298-13-80253, Max Pressure Limit 350bar, 06/19/14, APB
                   *For Use with G1367B Autosampler, 08/15/13, APB
```

Current Chromatogram(s)

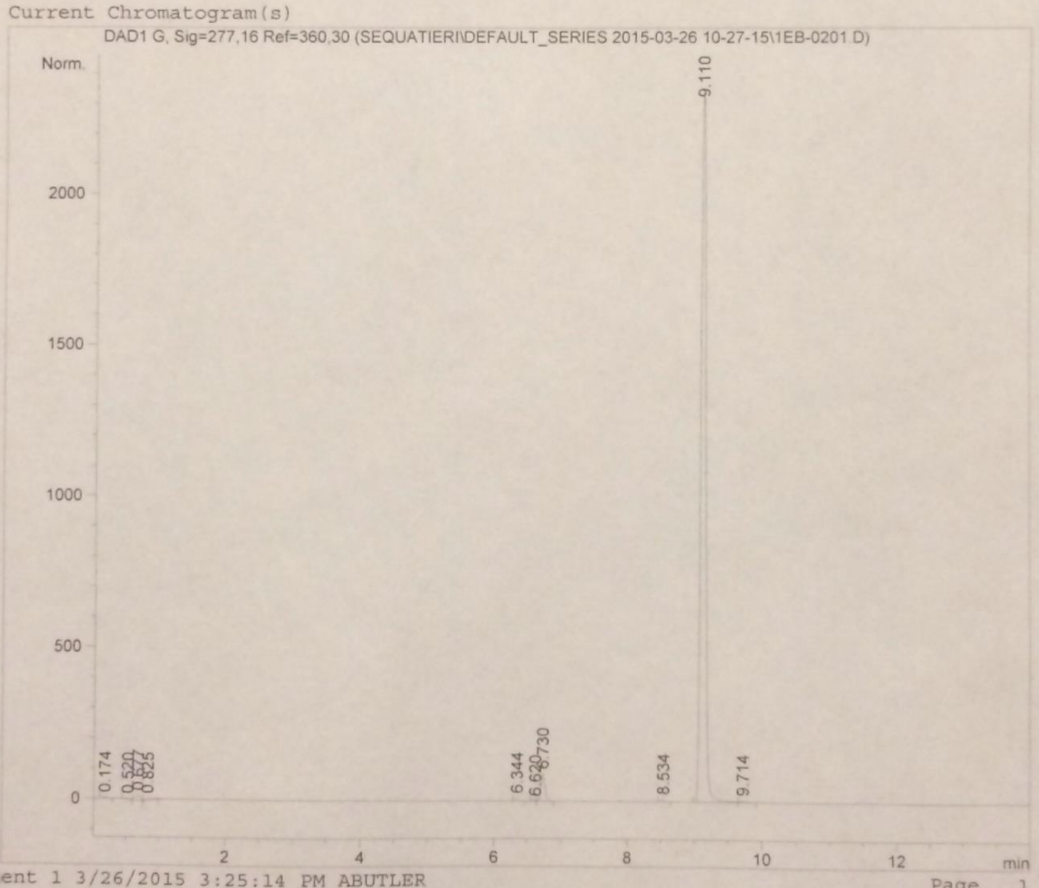

Instrument 1 3/26/2015 3:25:14 PM ABUTLER

Page 1 of 1

Print of window 80: MS Spectrum
Data File : C:\CHEM32\1\DATA\SEQUATIERI\DEFAULT_SERIES 2015-03-26 10-27-15\1EB-0201.D
Sample Name : SQ-8

Acq. Operator : sequatieri Seq. Line : 2
Acq. Instrument : Instrument 1 Location : P1-E-02
Injection Date : 3/26/2015 10:42:54 AM Inj : 1
Inj Volume : 2 µl
Acq. Method : C:\Chem32\1\DATA\SEQUATIERI\DEFAULT_SERIES 2015-03-26 10-27-15\ACID_GRAD_SERIES.M
Last changed : 6/19/2014 11:31:36 AM by ABUTLER
Analysis Method : C:\CHEM32\1\DATA\SEQUATIERI\DEFAULT_SERIES 2015-03-26 10-27-15\1EB-0201.D\DA.M (ACID_GRAD_SERIES.M)
Last changed : 6/19/2014 11:31:36 AM by ABUTLER
Method Info : Method: APB_ACID_GRAD_SERIES.M, multi-sample, 18 minutes run time/sample
2uL injection with 10sec Needle Wash (flushport) for LC-MS, ESI+/-, m/z 180-1200
Use with Sequence DEFAULT_SERIES.S, tune file: atunes_dual_fast.TUN
A1 H2O 0.1% FA, B1 95%ACN/5%H2O w0.1%FA,
0.3ml/Min gradient, 8 minutes, 30oC, Column 1
*For Use with ES Ind. Epic C18 MSO, 2.3u, 150A, 5cmx2.1mm column, S/N: 298-13-80253, Max Pressure Limit 350bar, 06/19/14, APB
*For Use with G1367B Autosampler, 08/15/13, APB

MS Spectrum

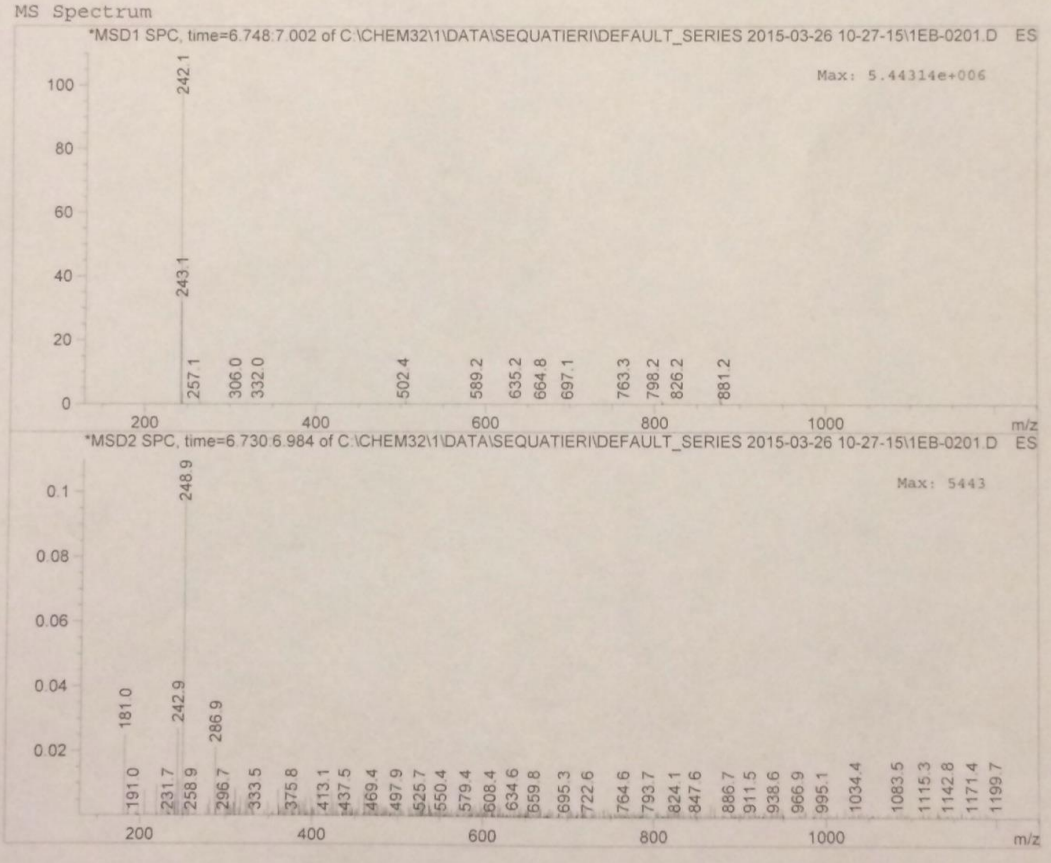

Instrument 1 3/26/2015 3:25:47 PM ABUTLER Page 1 of 1

LCMS output for Compound A

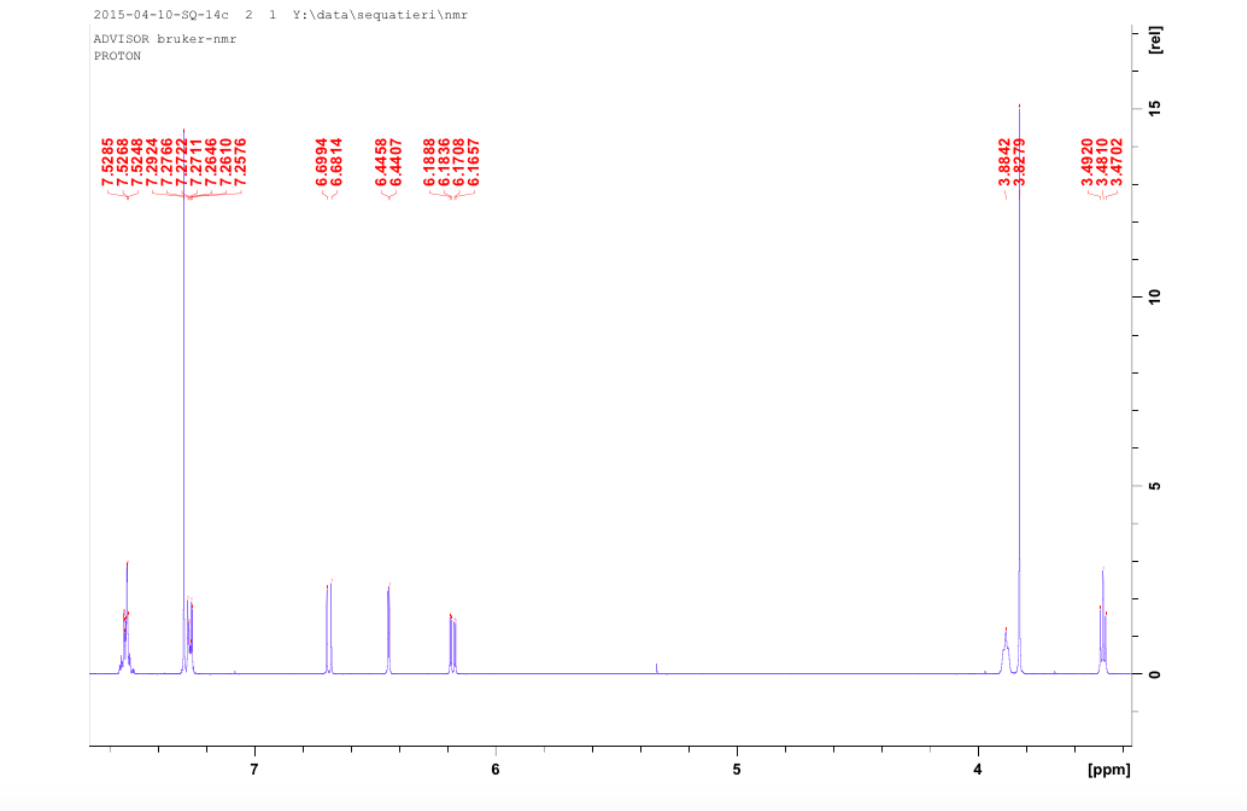

NMR of Compound B

Print of window 80: MS Spectrum
Data File : C:\CHEM32\1\DATA\SEQUATIERI\DEFAULT_SERIES 2015-03-26 10-27-15\1EF-0601.D
Sample Name : SQ-14

Acq. Operator : sequatieri Seq. Line : 6
Acq. Instrument : Instrument 1 Location : P1-E-06
Injection Date : 3/26/2015 11:43:58 AM Inj : 1
Inj Volume : 2 µl
Acq. Method : C:\Chem32\1\DATA\SEQUATIERI\DEFAULT_SERIES 2015-03-26 10-27-15\ACID_GRAD_SERIES.M
Last changed : 6/19/2014 11:31:36 AM by ABUTLER
Analysis Method : C:\CHEM32\1\DATA\SEQUATIERI\DEFAULT_SERIES 2015-03-26 10-27-15\1EF-0601.D\DA.M (ACID_GRAD_SERIES.M)
Last changed : 6/19/2014 11:31:36 AM by ABUTLER
Method Info : Method: APB_ACID_GRAD_SERIES.M, multi-sample, 18 minutes run time/sample
2uL injection with 10sec Needle Wash (flushport) for LC-MS, ESI+/-, m/z 180-1200
Use with Sequence DEFAULT_SERIES.S, tune file: atunes_dual_fast.TUN
A1 H2O 0.1% FA, B1 95%ACN/5%H2O w0.1%FA,
0.3ml/Min gradient, 8 minutes, 30oC, Column 1
*For Use with ES Ind. Epic C18 MSO, 2.3u, 150A, 5cmx2.1mm column, S/N: 298-13-80253, Max Pressure Limit 350bar, 06/19/14, APB
*For Use with G1367B Autosampler, 08/15/13, APB

MS Spectrum

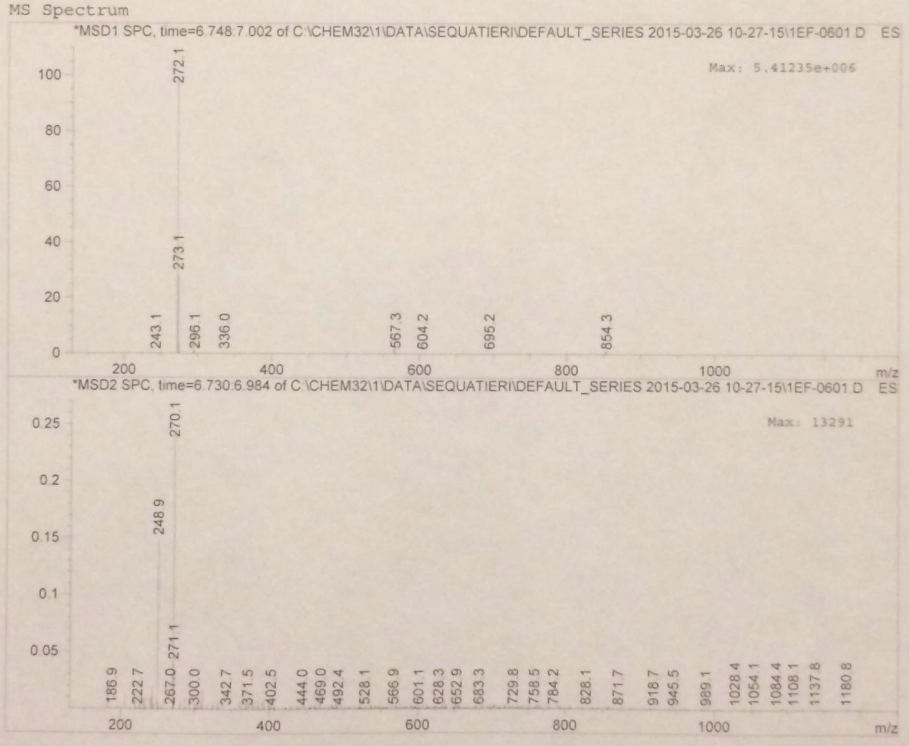

Instrument 1 3/26/2015 3:33:55 PM ABUTLER Page 1 of

LCMS of Compound B

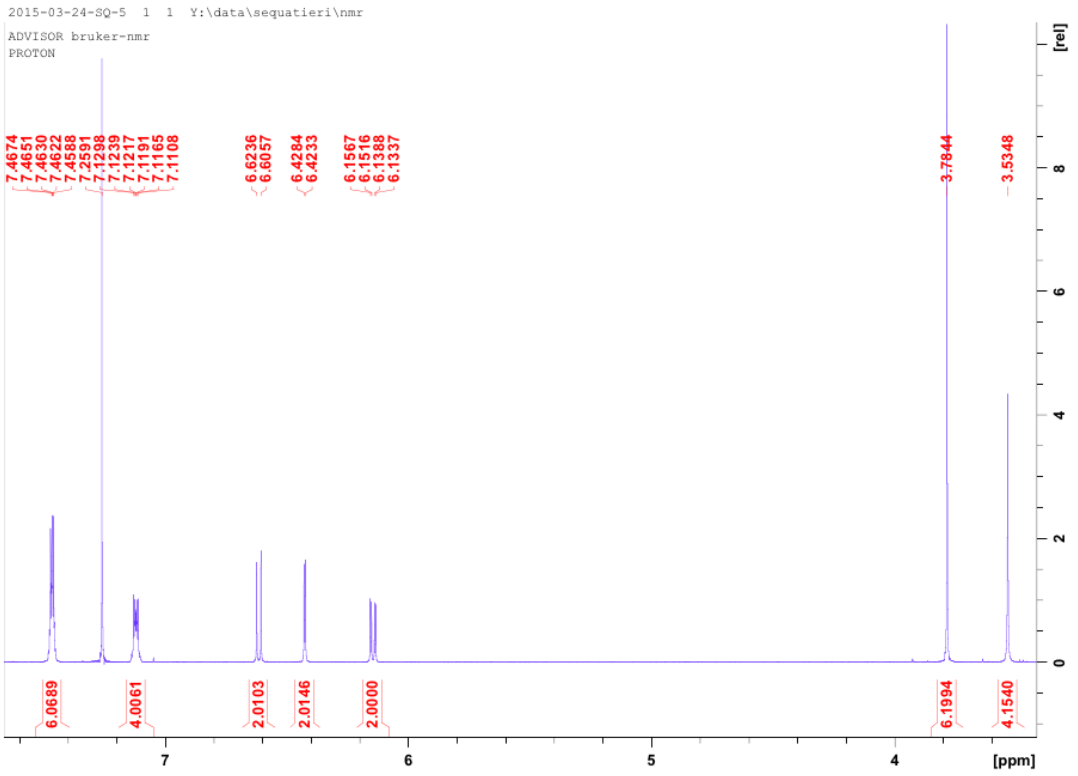

NMR of Compound C